Impacts of Current and Projected Oil Palm Plantation Expansion on Air Quality Over Southeast Asia

Sam J. Silva[1], Colette L. Heald[1], Jeffrey A. Geddes[2], Kemen G. Austin[3], Prasad S. Kasibhatla[3], Miriam E. Marlier[4]

[1]Department of Civil and Environmental Engineering, Massachusetts Institute of Technology, Cambridge, MA, USA
[2]Department of Physics and Atmospheric Science, Dalhousie University, Halifax, Nova Scotia, Canada
[3]Nicholas School of the Environment, Duke University, Durham, NC, USA
[4]Department of Ecology, Evolution and Environmental Biology, Columbia University, New York, NY, USA

Correspondence to: Sam Silva (samsilva@mit.edu)

Abstract. Over recent decades oil palm plantations have rapidly expanded across Southeast Asia (SEA). According to the United Nations, oil palm production in SEA increased by a factor of 3 from 1995 to 2010. We investigate the impacts of current (2010) and near-term future (2020) projected oil palm expansion in SEA on surface-atmosphere exchange and the resulting air quality in the region. For this purpose, we use satellite data, high-resolution land maps, and the chemical transport model GEOS-Chem. Relative to a no oil palm plantation scenario (~1990), overall simulated isoprene emissions in the region increase by 13% due to oil palm plantations in 2010 and a further 11% in the near-term future. In addition, the expansion of palm plantations leads to local increases in ozone deposition velocities of up to 20%. The net result of these changes is that oil palm expansion in SEA increases surface O_3 by up to 3.5 ppbv over dense urban regions, and in the near-term future could rise more than 4.5 ppbv above baseline levels. Biogenic secondary organic aerosol loadings also increase by up to 1 $\mu g\ m^{-3}$ due to oil palm expansion, and could increase a further 2.5 $\mu g\ m^{-3}$ by in the near-term future. Our analysis indicates that while the impact of recent oil palm expansion on air quality in the region has been significant, the retrieval error and sensitivity of the current constellation of satellite measurements limit our ability to observe these impacts from space. Oil palm expansion is likely to continue to degrade air quality in the region in the coming decade and hinder efforts to achieve air quality regulations in major urban areas such as Kuala Lumpur and Singapore.

1. Introduction

Palm Oil is currently the most popular source of food oil in the world, and is rapidly gaining importance as a source of biofuel (Corley, 2009). Over 80% of global palm oil production takes place in Southeast Asia (SEA), with more than 10 million hectares of land farmed in 2005 (Fitzherbert et al., 2008). According to the Food and Agriculture Organization of the United Nations (faostat3.fao.org), palm oil production in SEA has grown by a factor of 5 over the past 20 years. By 2020, the total area occupied by oil palm plantations in SEA is expected to increase even further (Austin et al. 2015, Marlier et al. 2015b). This represents a significant and rapid change in land use over a relatively small region. The palm expansion in SEA

is just one example of land use change that may drive changes in atmospheric composition; however, to date there has been limited exploration of these impacts (Heald and Spracklen, 2015).

The impact of oil palm expansion on global carbon stocks and biodiversity has been studied extensively. Austin et al. (2015) suggest that up to 47 MtC yr^{-1} will be emitted due to oil palm land use change in Kalimantan alone from 2010-2020. Carlson et al. (2013) estimate that the plantations could generate over 25% of Indonesia's projected carbon emissions by 2020. Furthermore, replacing native forests with oil palm has and will continue to threaten biodiversity across the region. Fitzherbert et al. (2008) found that only 15% of all species present in the natural forest were also found in oil palm plantations.

This rapid land use change across SEA has also altered surface-atmosphere exchange of trace gases over the region, with potential implications for regional air quality. Airborne observations over northeastern Borneo during the 2008 OP3 campaign indicated that oil palm plantations emit 7 times more isoprene than the nearby rainforest (Hewitt et al., 2010). Isoprene is the most abundant volatile organic compound (VOC) emitted by plants, is a precursor of secondary organic aerosol (SOA), and can play an important role in surface ozone formation, depending on the local chemical environment. Despite this dramatic increase in isoprene emissions, no appreciable difference in surface O_3 over palm versus native forest was observed during OP3 (Hewitt et al., 2009). Growth of oil palm plantations also impacts the deposition of gases and particles from the atmosphere due to changes in the total amount of plant surface area available for deposition. The OP3 observations show that deposition velocities of ozone over oil palm are half the magnitude of deposition velocities over the natural forest (Fowler et al., 2011). Fowler et al. (2011) suggest that this is due to smaller non-stomatal exchange of ozone from the oil palm canopy. Expansion of oil palm may also impact soil NO_x emissions due to fertilizer application, changing land types, changes in the amount of NO that escapes through the canopy, and changes in the amount of sunlight that reaches the ground (Hewitt et al., 2009). The links between these rapid land use changes and air quality become even more important in light of the tremendous population growth and significant air quality problems already present throughout SEA. The region contains more than 570 million people, an increase of more than 10% since 2000 (United Nations Population Division, 2011). Forouzanfar et al. (2015) found that indoor and outdoor atmospheric pollution are both within the top 10 leading risk factors for premature mortality throughout SEA.

The impact of oil palm plantations on air quality has been investigated in previous modeling studies. Warwick et al. (2013) simulate the influence of modern day oil palm distributions over Borneo, constraining both isoprene and NO_2 fluxes to values measured during the OP3 campaign, and converting the entire island of Borneo to oil palm plantations. They find the potential for up to 70% (30-45 ppbv) increases in regional O_3 concentrations. Ashworth et al. (2012) use the HadGEM2 model to assess the impact of biofuel feedstocks on air quality. Part of their study included oil palm plantations in SEA, where they scaled forest emissions to meet the observed plantation emissions. They found that the oil palm-related increase

in isoprene emissions by 2020 could lead to local increases in surface O_3 and SOA of up to 3 ppbv and 0.4 μg m^{-3}, respectively.

Agricultural burning across SEA (partially related to palm oil production) is an additional source of air pollution in the region. Marlier et al. (2015b) assessed different land use scenarios across Sumatra to determine their overall influence on current and future fire emissions. They found that the scenario with the highest amount of oil palm had the largest associated fire emissions (100 Tg DM yr^{-1}); these fires contribute up to 60% of the total smoke concentrations across equatorial SEA.

In this study, we use the GEOS-Chem model to simulate the potential impacts of oil palm on air quality broadly across SEA for current and future oil palm expansion scenarios. We go beyond previous studies by explicitly simulating the concurrent perturbations to biogenic emissions, soil NO_x emissions, and dry deposition, and exploring the net impacts on air quality in the region. We compare these results with available satellite observations to investigate whether the current constellation of satellite instruments can detect the changes in air quality driven by rapid land use change.

2. Model Description

2.1 The GEOS-Chem model

We use the global chemical transport model GEOS-Chem v9-02 (www.geos-chem.org) to investigate the changes in air quality associated with oil palm plantations in SEA. The model is driven by assimilated meteorology from the Goddard Earth Observing System (GEOS). We use GEOS-5 meteorology for the year 2006 in all of our simulations, due in part to the availability of updated anthropogenic emission inventories for this year. For this analysis, we perform a series of nested simulations of GEOS-Chem over the Asian domain (70˚–150˚E, 10˚S–55˚N) at 0.5˚x0.667˚ horizontal resolution with 47 vertical layers. Boundary conditions are produced using the same version of the global model at 2˚x2.5˚ horizontal resolution. The model was initialized with a 1-year simulation at 2˚x2.5˚ horizontal resolution, and then an additional 6-month simulation at 0.5˚x0.667˚. A map of the Asian domain, and the region of particular interest to this study is shown in Figure 1.

The GEOS-Chem oxidant-aerosol simulation includes H_2SO_4-HNO_3-NH_3 aerosol thermodynamics (Park et al., 2006; Pye et al., 2009) coupled to a detailed HO_x-NO_x-VOC-O_3-BrO_x chemical mechanism (Bey et al., 2001; Mao et al., 2013). Secondary organic aerosol (SOA) is produced from the oxidation of biogenic hydrocarbons (isoprene, monoterpenes, and sesquiterpenes), aromatics, and IVOCs and represented with a volatility basis set approach (Pye et al., 2010; Pye and Seinfeld, 2010).

The global simulations are driven by anthropogenic emissions from the Emissions Database for Global Atmospheric Research version 3 (EDGARv3), including emissions from ship exhaust (Olivier et al., 2001). Over the Asian region, a more recent anthropogenic emission inventory from the year 2006 is used (Streets et al., 2003, 2006). Geddes et al. (2015b) show that the long-term (1996-2012) trend in satellite-derived estimates of ground-level NO_2 concentrations over SEA is relatively

5   small, indicating that regional changes in anthropogenic emissions are not large. Global emissions from aviation are based on the AEIC inventory (Stettler et al. 2011, Simone et al. 2012). Biomass burning emissions for 2006 follow the GFED3 inventory (van der Werf et al., 2010). We note that the GFED3 emissions indicate that 2006 was a higher than average fire year in the region. Additional simulations using emissions and meteorology from 2007 and 2008 indicate that the choice of model year does not substantially influence the results of this work, spatial patterns are all consistent and concentration

10   changes are all less than 10%.

The GEOS-Chem land use module developed by Geddes et al. (2015a) is used to drive surface-atmosphere exchange processes in the model. Land use is described using 16 plant functional types (PFTs), with an associated monthly leaf area index (LAI) per PFT. The baseline global PFTs and associated LAI are from the year 2000 inputs to the Community Land

15   Model v.4 (http://www.cgd.ucar.edu/tss/clm), which are based on satellite observations (Lawrence et al., 2011). The dominant vegetation types in SEA are plotted in Figure 2. Biogenic emissions of VOCs (BVOCs) are calculated online for each PFT following MEGANv2.1 (Guenther et al., 2012). These BVOC emissions respond to temperature, available sunlight, leaf area index, leaf age, and soil moisture. These responses are quantified as activity factors which are applied to the basal emission factor to calculate emissions that vary with meteorology and phenology. Dry deposition is calculated

20   following Wesely (1989). The depositional velocity is a function of the aerodynamic, boundary layer, and canopy resistances, added in series. The aerodynamic resistance depends on atmospheric stability and surface roughness height, the boundary layer resistance is a function of the chemical species and meteorology, and the canopy resistance varies with the chemical properties of the deposited species and the land type. To calculate the canopy resistance, land types are mapped from the 16 PFTs to the 11 depositional surfaces described in Wesely (1989). For the calculation of the aerodynamic and

25   canopy resistances, we take into account the influence of LAI on the land properties. We account for all depositional surface types within a grid cell by preserving the fractional land cover of each grid box. Soil NO_x emissions are a function of soil moisture, temperature, available nitrogen, and land use type and are calculated following Hudman et al. (2012). The land types for these emissions are mapped from the PFTs to 24 biomes described in Steinkamp and Lawrence (2011). Additionally, a canopy reduction factor, to account for the loss of NOx within the canopy, is calculated as a function of LAI

30   and meteorological parameters.

GEOS-Chem has previously been used to study air quality in SEA. Trivitayanurak et al. (2012) use the nested model to better understand the distribution and sources of atmospheric trace constituents over Asia. They find that the model captures the vertical and spatial variability of trace constituents such as CO, isoprene, and sulfate to within 30% of observations from

several aircraft campaigns. They also note that the model under predicts AOD as measured by MODIS, which they attribute to an underestimate of local biogenic SOA. Fu et al. (2007) use the model in combination with satellite measurements of formaldehyde to constrain non-methane VOC emissions broadly across Asia from 1996-2001. They show that observed and modeled HCHO are highly correlated in the region. Jiang et al. (2015) compare the model and satellite estimates of CO, O_3,

5 and NO_2 in Asia, and conclude from these comparisons that the GEOS-Chem simulation of tropospheric O_3 is reliable within the Asian domain.

2.2 Description of SEA land use

To account for oil palm plantations, we add a new plant functional type to the land module to calculate palm specific biogenic emissions, soil NO_x emissions, and dry deposition. The basal isoprene emission factor of oil palm is set to the basal

10 rate of 7.8 mg m^{-2} h^{-1} measured during OP3 (Misztal et al., 2011); this basal emission factor is modulated online by local meteorology and phenology to estimate emissions. Previous studies scaled modelled emissions of Broadleaf Evergreen Trees (Ashworth et al., 2012), or kept these emissions fixed to the measured rate during OP3 (Warwick et al., 2013). The basal isoprene emission factor of the native forests (considered to be broadleaf evergreen tropical trees) is reduced to 1.6 mg m^{-2} h^{-1} to match the OP3 measurements (Langford et al., 2010), which is a factor of 4 lower than the emission factors for

15 broadleaf evergreen tropical trees within MEGANv2.1, and consistent with the rainforests of Southeast Asia emitting less isoprene than South American and African rainforests. This difference is likely due to a previous dearth of measurements across the rainforests of SEA to constrain MEGANv2.1 (Guenther et al., 2006; Guenther et al., 2012). Observations suggest that oil palm is not a significant emitter of monoterpenes and sesquiterpenes, but the mechanisms behind this are not clear (Misztal et al., 2011). The observations of Misztal et al. (2011) do indicate that oil palm plantations have higher emissions of

20 estragole and toluene. However their impact on atmospheric chemistry and composition is not well constrained, and Guenther et al. (2012) indicate that emissions of these species are relatively small, particularly as compared to isoprene. In light of this, and the large uncertainties on the estimates of basal emissions for these other biogenic compounds from natural forests in the region, we modify only the emission factor of isoprene for oil palm relative to background forests.

25 During the OP3 campaign Fowler et al. (2011) observed that relatively few of the oil palm plantations were fertilized. When extrapolated across the whole expanse of oil palm plantations, it was found that the average soil NO_x emission of plantations is similar to that of the background forest. In addition, we have no information on the relative impacts of palm plantations and natural tropical forests on nitrogen cycling in the soil. Therefore, the biome type-specific soil NO_x emissions parameters for oil palm are identical to the tropical forest conditions in our simulations.

The leaf area index (LAI) of an oil palm plantation changes as the trees age. Oil palms themselves live for more than a decade, and their leaves live for 600-700 days; this contributes to LAI values that can vary from 2 to 8 in mature plants (Van Kraalingen et al., 1989). Oil palm LAI is set to 4.5 for these simulations; this value is selected as an approximation of the

average over the lifespan of the plant (Van Kraalingen et al., 1989), and therefore a likely average for the plantation as a whole. We explore the sensitivity of our results to this specified LAI value in Section 3. For the Wesely depositional scheme land types, oil palm is assumed to be most similar to the native forest, as opposed to the "crop" land type. This assumption is made simply because oil palm plantations are physically much closer to a tall tree forest than a wheat field or cornfield. We

5   do not attempt to model the detailed growth, harvesting, and senescence history of the plantation (Fan et al., 2015). Previous studies (Ashworth et al. 2012, and Warwick et al. 2013) did not explicitly simulate the concomitant changes to deposition due to oil palm expansion. They instead performed short sensitivity studies wherein Warwick et al. (2013) doubled the modelled deposition velocities, and Ashworth et al. (2012) scaled modelled deposition parameters (roughness length and LAI) by observed canopy height and biomass density.

Several land use maps are used to describe the modern and future distribution of oil palm over SEA (Figure 3). For the modern day scenario, we use a land use map developed by Miettinen et al. (2012), which describes land use across insular SEA (-10˚ N to 10˚N, 95˚E to 140˚ E) in 2010 on a 250 meter grid, and includes a land classification for palm plantations. The future expansion scenario maps are adapted from Marlier et al. (2015b) and Austin et al. (2015). Marlier et al. (2015b)

15 developed a variety of scenarios at 1km resolution to understand changes in fire emissions associated with land use change in Sumatra. We use the "High oil palm" scenario to represent a realistic upper limit on the 2020 distribution of Sumatran oil palm. This map was reported originally as the probability that a given grid box will contain oil palm in 2020. The probability for each grid box was treated as the percent area covered by palm, and converted to fractional PFT coverage at the 0.23˚x0.31˚ resolution that is input into the GEOS-Chem land module. This leads to an increase of 112% in total palm

20 coverage in Sumatra from 2010 to 2020. Austin et al. (2015) mapped the future oil palm distribution in Kalimantan (Indonesian Borneo) using a logistic regression model at 250 meter resolution to understand the impact that oil palm could have on emissions of CO_2. We constrained that logistic regression model to a total of 3.6Mha of oil palm expansion to create a map for the 2020 distribution of oil palm in Kalimantan, following the totals given by Austin et al. (2015). This leads to an increase of 108% in total palm coverage over Kalimantan from 2010 to 2020. Note that these two datasets cover only

25 Sumatra and Kalimantan, which together represent 54% of palm production in the region in 2010, but much of the available land for future expansion. From 2010 to 2020 oil palm production in these two regions increase by 10.8 Mha. Our projections do not consider the potential oil palm expansion in the rest of the SEA region. For both scenarios, the oil palm plantations are added as a land type and fractional coverage of all pre-existing vegetation classes from the base land map are reduced accordingly. This differs from previous studies where Warwick et al. (2013) assumed the entire island of Borneo

30 was covered in oil palm plantations, and Ashworth et al. (2012) did not consider any changes to the underlying vegetation characteristics, instead they scaled isoprene emissions from selected tropical broad-leaved trees. It is important to note that the 2020 distribution used here is the best estimation of a near-term future wherein large increases in oil palm plantations continue to occur. The distribution may not be an accurate prediction for the specific year 2020. It is meant to represent a realistic near-term scenario, and for this reason we refer to it from here on as the "future" distribution.

3. Impacts of palm expansion on air quality in Southeast Asia

To understand the overall air quality impact of oil palm plantations in SEA, we explore three major plantation scenarios. The first uses a land map with no palm to establish a baseline. This simulation is referred to as "No Palm" and is representative of conditions that pre-date the major palm expansion in SEA (~1990). The next is a simulation we call "Modern Palm", using the 2010 distribution from Miettinen et al. (2012). The third simulation is "Future Palm," and uses the merged land maps from Marlier et al. (2015b) and Austin et al. (2015) for Sumatra and Kalimantan. In addition, we perform sensitivity scenarios for the Modern Palm distribution to disaggregate land use change-driven impacts on BVOC emissions from dry deposition and soil NOx emissions; this is referred to as "BVOC-only". Results are shown here for annual means; seasonal differences are minor.

3.1 Changes in Surface-Atmosphere Exchange

The direct influence of oil palm plantation expansion is on surface-atmosphere exchange, most significantly BVOC emissions and dry deposition.

The changes in BVOC emissions are as anticipated: where palm is added, surface fluxes of BVOCs increase. By far the largest increase is that of isoprene. There are increases in other BVOCs due to replacement of unforested regions (wetlands, pastureland, etc.) with oil palm, but they are at least a full order of magnitude smaller than the concomitant changes in isoprene. Figure 4 shows the increase in isoprene emissions associated with the addition of oil palm plantations in both the Modern and Future scenarios, compared to the baseline No Palm scenario. The largest increases in isoprene emissions in the Modern Palm scenario occur in northern Borneo, Sumatra, and the southern Malay Peninsula. This addition of palm increases isoprene emissions by a factor of three over northeastern Borneo, where the OP3 campaign took place (see section 4). This growth corresponds to an absolute increase on the order of 14 μmol m^{-2} hr^{-1}. The largest relative changes in isoprene emissions occurred over the northern half of Sumatra and the southern Malay Peninsula, with up to a 4.5 fold increase over the simulation without oil palm. Similar to northeastern Borneo, the absolute change in emissions is on the order of 10 μmol m^{-2} hr^{-1}. Sumatra and the Malay Peninsula are of particular importance due to their proximity to the large urban centers of Kuala Lumpur and Singapore. Oil palm plantations in 2010 result in an additional 1.26 TgC yr^{-1} of isoprene emission from SEA, a 13% increase from the No Palm scenario.

The Future Palm emission scenario changes are limited to Sumatra and Kalimantan (Indonesian Borneo) as prescribed in the land use change scenarios considered (Section 2.2). Isoprene emissions in Kalimantan increase by a factor of 2 (~10.6 μmol m^{-2} hr^{-1}) from the No Palm simulation. These are mostly regions that are as yet undeveloped and are good candidates for future palm agriculture. There are many regions in Sumatra where the changes in isoprene emissions are greater than a factor of 3-4, with an absolute difference in excess of 14 μmol m^{-2} hr^{-1}. Similar to the changes in the Modern Palm scenario, these

isoprene emissions increases are very near large urban regions. In this scenario, the total change in isoprene emissions from 2010 to the near-term future scenario in SEA is 1.1 TgC yr^{-1} across SEA, a 10% increase in isoprene emissions. This emission increase is nearly twice as high as previous work (Ashworth et al., 2012), due to differences in the assumed future distribution of oil palm.

The impacts of oil palm expansion on dry deposition velocities are more complex than the BVOC emissions changes. As stated in Section 2.2, LAI influences the resistance terms in the calculation of depositional velocities, and oil palm plantations tend to have a higher LAI (prescribed here to a fixed value of 4.5) than both the natural forest (ranges from 0 to 6.77, with a median value of 4 for SEA), and grasslands or previously cleared agricultural lands. The LAI for the various scenarios is shown in Figure 5. The addition of oil palm plantations increases the LAI for much of SEA. For a highly reactive species such as O_3, an increase in LAI directly leads to an increase in the depositional velocity over that surface, as seen in Figure 6. It should be noted that there are minor perturbations to the deposition of other gas phase species as well. However, O_3 deposition is most sensitive to this land use change due to its high reactivity and strong LAI dependence. The impact of oil palm expansion on particle deposition is negligible.

Modern palm distributions increase O_3 dry deposition velocities most significantly in the Malay Peninsula and North Sumatra. In both regions, the largest changes are increases of 0.05 cm s^{-1}, or nearly 15%. This change is the opposite sign and smaller in magnitude than the measured difference in O_3 deposition velocity across the forest to palm transition reported by Fowler et al. (2011); however our values are not directly comparable to those measurements given the heterogeneity of land types within each grid cell, the resolution of the model, and the fact that the simulated depositional velocity changes are an aggregate of many land types transitioning to oil palm plantations (not purely forest to palm). Figure 5 shows that the Malay Peninsula and North Sumatra exhibit the largest changes in deposition partially due to the dense palm plantations in the region, and also due to the large changes in LAI due to those plantations replacing cleared land, low LAI forests, and other varied land types. Across SEA, the overall impact of palm plantations on ozone deposition is small, with a net 0.5% increase in O_3 depositional velocity.

The future distribution of oil palm produces the largest changes in ozone dry deposition velocities over Kalimantan, and again Sumatra (Figure 6). In both these regions, increases in deposition velocities are as large as 0.06 cm s^{-1}, or 20% relative to the No Palm scenario. As with the Modern Palm scenario, the most significant changes occur over areas where oil palm plantations replace cleared lands. The average change in ozone dry deposition fluxes across the region from no Palm to the future scenario is an increase of 1.0%.

In this work, the basal emission of soil NO_x in oil palm plantations is identical to that in natural forests. However the loss of NO_x to the canopy is impacted by differences in LAI. We find that there are negligible changes in the net soil NO_x emission

over regions where the land transitioned from forest to palm. This is largely consistent with the OP3 field campaign observations (Fowler et al., 2011), which indicated that few of the palm plantations are fertilized. The soil NO_x changes are more significant where other land type changes occurred; for instance, moving from pastureland to oil palm. However there remains substantial uncertainty surrounding fertilization practices in SEA palm plantations. Therefore, this simulated perturbation in soil NO_x emissions is likely a lower limit. Additional small changes in the re-emission of nitrogen occur as a feedback related to changes in the total amount of nitrogen deposited from the atmosphere.

LAI sensitivity tests indicate that assigning oil palm plantation LAI from 3 to 6, as opposed to the 4.5 used in our simulations, has modest impacts on the changes in surface-atmosphere exchange over this region. Lower LAI reduces isoprene emissions and dry deposition, and increases soil NOx emissions broadly across oil palm regions by ~5% compared to the Modern Palm simulation. The inverse is true of higher LAI values. The maximum changes in these processes are of order 10% relative to the Modern Palm simulation.

3.2 Changes in Air Quality

Atmospheric composition over SEA is impacted by oil palm plantation expansion via the perturbations in surface-atmosphere exchange discussed in Section 3.1. We focus here on how these changes connect to surface air quality in the region.

Formaldehyde (HCHO) is an oxidation product of isoprene, a toxic pollutant, and an O_3 precursor. Figure 7 shows the sensitivity of simulated HCHO to changes in the oil palm distribution. The largest increases in surface HCHO due to Modern Palm are in regions where surface fluxes of isoprene change the most, and are locally isolated due to the short atmospheric lifetime of HCHO (~hours). The largest relative increases in HCHO (up to 70%) are seen over northeastern Borneo, while concentrations near the urban centers on the Malay Peninsula show increases greater than 50%. In terms of absolute values, the largest changes occur over Sumatra, with surface values increasing by as much as 2 ppbv. The increase over northeastern Borneo is lower, at around 1.4 ppbv. Across SEA, mean surface HCHO increases by 1.6%. HCHO sensitivities to Future Palm distributions share similar spatial characteristics to the Modern Palm scenario, with more pronounced changes over Kalimantan. Fractionally, the largest changes are in Sumatra, where surface concentrations of HCHO increase by up to a factor of 1.8 compared to the No Palm baseline. Mean surface HCHO concentrations over SEA increase by 2.8% compared to the No Palm baseline. Absolute changes in surface HCHO are still quite high over Sumatra, above 2.5 ppbv in many regions.

Figure 8 shows that the simulated response of surface NO_x to the oil palm expansion is very small. In principle, this response is influenced by changes to deposition, soil NO_x emissions, and isoprene fluxes. Given the modest difference in deposition and soil NO_x emissions, the dominant impact is the elevated concentrations of isoprene. Additional isoprene leads to more

conversion of NO to NO_2, and therefore increases the formation of HNO_3, leading to a net loss of NO_x. This effect is only apparent across the southern Malay Peninsula, a region with high surface NO_x concentrations, due in large part to significant anthropogenic activity. These changes are typically less than 0.1 ppbv, on the order of 5% decreases. The Future oil palm simulation shows similar decreases in the surface NO_x response. These decreases are as large as 1 ppbv over Sumatra, a 5% drop. There is a decrease in NO_x across Kalimantan on the order of ~0.5 ppbv related to the same chemistry. In reality, these changes may be dwarfed by the impact of anthropogenic emissions of NO_x associated with production and processing facilities as well as oil palm fertilization; these changes are highly uncertain, and have not been included here.

The introduction of oil palm and the resulting increase in concentrations of isoprene can lead to changes in concentrations of ozone through VOC-NO_x chemistry. At the same time, the increase in the deposition velocity of ozone leads to a shorter average lifetime, which decreases concentrations. In our modeled responses we see both of these signatures across SEA. Figure 9 shows that the surface ozone response to Modern Palm is most prominent over the southern Malay Peninsula (up to 4 ppbv), with changes over northeastern Borneo and Sumatra as well. Over the Malay Peninsula and Sumatra, a region not sampled during OP3, surface ozone concentrations increase by up to 26% (3-4 ppbv) due to palm expansion. Ozone formation is enhanced in these regions, where additional isoprene emissions combine with NO_x rich air near the major urban centers. Surface ozone increases in northeastern Borneo are on the order of 2 ppbv, located in the near vicinity of the oil palm plantations. These results differ spatially from Warwick et al. (2013), likely due to the substantially different land maps used for oil palm emissions of VOCs over Borneo. Hewitt et al. (2009) did not observe a change in surface O_3 concentrations due to oil palm at all over northeastern Borneo. Much of the discrepancy between our results and the Hewitt et al. (2009) observations can likely be explained by sampling and the different spatial resolution of the measurements and the model. The 0.5˚x0.666˚ grid box resolution used in this study is on the order of the entire study region for OP3.

Adding oil palm plantations usually increases the LAI (Figure 5), leading to an increased depositional velocity (Figure 6), which ultimately results in an increased sink of O_3. However, this is generally counteracted by the large increase in isoprene emissions. Our BVOC-only sensitivity simulation indicates that the changes in biogenic emissions are the dominant factor controlling the changes in O_3. The ratio of the changes in the Modern Palm simulation to those in the BVOC-only simulation is shown in Figure 10. Across most of the region, this ratio is nearly 1, indicating that the changes in soil NO_x and deposition have little impact on O_3. That said, over regions that undergo large forest to palm transitions and have relatively low background O_3 concentrations, such as Indonesian Borneo, up to 50% of the O_3 change is related to dry deposition and soil NO_x. A small decrease in the annual average O_3 concentrations (~10 pptv) is simulated over southwestern Borneo, where under low-NOx conditions, the additional isoprene from palm consumes O_3.

The changes in surface ozone are exacerbated in the Future Palm scenario (Figure 9). The relative near-term future surface concentrations over the Malay Peninsula increase by up to 4.5 ppbv (25%) over the No Palm scenario. This is larger than the

impact (<1 ppbv) estimated by Ashworth et al. (2012), likely due to their more modest future estimate of palm expansion. O_3 concentrations in southern Kalimantan increase by up to 1 ppbv (~5%).

These changes have substantial impacts on local urban air quality in Kuala Lumpur and Singapore, which aim to adhere to the World Health Organization (WHO) (http://www.who.int/) guidelines for the daily maximum 8-hr average ozone not to exceed 50 ppbv. The number of days per year which exceed this standard in our simulation are shown in Figure 11 for both Singapore and Kuala Lumpur. The No Palm simulation suggests that surface O_3 exceeds the WHO standard for 35 days in Singapore and 23 days in Kuala Lumpur. We show how additional isoprene emissions associated with palm expansion increases O_3 concentrations in these urban regions, exacerbating air quality issues. In particular, over Kuala Lumpur, Modern Palm is associated with 33 additional days of O_3 exceedance, increasing to 62 total days in the Future Palm scenario. The impacts over Singapore are more modest; nevertheless palm expansion is associated with 8 more days above the WHO guideline levels in the future scenario. From Figure 9, we observe that ozone air quality in Jakarta, another large urban center in the region, is relatively unaffected by oil palm expansion, due to the local transport patterns and the spatial distribution of the plantations.

The changes in biogenic secondary organic aerosol (SOA) all track very closely with HCHO and isoprene, due to the rapid formation of SOA from biogenic precursors. These changes are shown in Figure 12. Relative increases in surface biogenic SOA concentrations due to Modern Palm expansion are highest in northeastern Borneo and the southern Malay Peninsula, with increases larger than 60%, approximately 1 μg m^{-3}. Future palm expansion may lead to further substantial enhancements of SOA in the region, as high as 3.5 μg m^{-3} and generally at least 1.5 μg m^{-3} over regions with high oil palm density. Again, these values are larger than those in Ashworth et al. (2012), who employ a more modest oil palm expansion scenario. Palm expansion in the coming decade could lead to an average 5% increase in surface SOA across the region, degrading visibility and enhancing air pollution exposure. Though most of these changes are local, they do stretch into protected nature preserves and dense urban regions. Though these change to biogenic SOA are large, it is important to note that biogenic SOA is not the dominant source of particulate matter pollution across SEA. Marlier et al. (2013) show that regional fires can contribute to annual average particulate matter concentrations of more than 100 μg m^{-3}, several orders of magnitude higher than the changes in SOA related to oil palm plantations.

The changes in air quality are not as sensitive to the choice of palm LAI (between 3 – 6), as compared to the changes in surface-atmosphere exchange processes. The magnitude of the changes in HCHO, O_3, and NO_x are all on the order of 1%, and not more than 5% relative to the Modern Palm scenario. The relative changes in SOA are also generally small, but are slightly higher (~±8%) over the southern Malay Peninsula, near Singapore.

4. Limitations of Observing Systems for Detecting the Impacts of Land Use Change on Air Quality

There are no long-term surface measurements of air quality in SEA to assess and validate our simulated impacts of oil palm expansion, beyond the snapshots provided by the OP3 campaign discussed above. However, a suite of space-based instruments has been making global measurements during the peak of the palm expansion (2004 – Present). The rapid and extensive expansion of oil palm in SEA is arguably the most dramatic example of local land use change during the satellite era for atmospheric composition. We investigate whether the anticipated changes in air quality have been detectable from space over the last decade. We focus on the record of HCHO, O_3, NO_2, and Aerosol Optical Depth (AOD) observations, the suite of observable species that may have been impacted by oil palm development, and we use our model simulation to direct this analysis.

All of the measurements analyzed here are part of the A-Train constellation of polar-orbiting satellites. As such they provide daily coverage in a sun synchronous orbit, with local overpasses ~10:00 and ~13:00. We use HCHO, NO_2, and O_3 measurements from the OMI instrument on board the NASA/Aura satellite, which has been operating since late 2004. The satellite has a 14x24km footprint size. HCHO observations are from the NASA OMI HCHOv3 (OMHCHO) retrieval; filtering and quality control screening is described in Gonzalez Abad et al. (2015). These data have been used previously to successfully analyze large urban source regions and assess biogenic isoprene emissions (e.g. Zhu et al., 2014). We use the NO_2 retrievals from the DOMINOv2 retrieval product, as described in Boersma et al. (2011). These data have been used previously to assess emissions of NO_2 across Asia (Vinken et al., 2014). We use the NASA OMO3PR product (Bak et al., 2015) that retrieves a vertical profile of ozone concentrations in 18 layers extending from the surface up to 0.3 hPa. There are alternative satellite measurements of all the above chemical species, but we focus on this suite of measurements that provide a consistent record during the peak palm expansion, aboard the same observing platform. We also explore Aerosol Optical Depth (AOD) measurements from two MODIS instruments on board the NASA Terra and Aqua satellites. Our analysis uses the MODIS collection 6 product (Sayer et al., 2014).

All satellite data are filtered spatially to best capture the signal of palm expansion against the significant background of other sources. These include a large urban signature from the Kuala Lumpur, Singapore, and Jakarta megacities and substantial fire activity in both Sumatra and Indonesian Borneo. To address this, we focused our analysis on the remote northwest corner of Borneo, shown in the map of Figure 13. This contains the region where the airborne measurements were made during the OP3 campaign (Hewitt et al., 2010). Our model simulations suggest that this region has exhibited significant changes in air quality due to oil palm expansion, particularly in HCHO. Using Mientennen et al. (2010) as a base map, satellite measurements over potential palm plantation land types are identified within the "Palm" region, non-urban forest land-types in the "Forest" region, and ocean in the "Ocean" region. This classification allows for various time series analyses

to be performed over what should be three distinct emission and depositional land types, and thus best isolate the impact of oil palm on local air quality.

Of all the atmospheric constituents observed, changes in HCHO concentrations should represent the strongest air quality
5   perturbation due to oil palm expansion according to our model simulation (Figure 7). This is due to the strong local source of HCHO through oxidation of isoprene from oil palm, combined with the small urban sources in the region and the relatively constant background HCHO from methane oxidation. Background HCHO concentrations in our model simulation are on the order of 10^{16} molecules cm^{-2}. The background concentrations observed by the OMI instrument are also of the order 10^{16} molecules cm^{-2}. From our model simulations, the expected change in column concentration of HCHO due to Modern Palm
10 expansion is of order 10^{15} molecules cm^{-2}. OMI is most sensitive to regions with very high HCHO concentrations ($> 2 \times 10^{16}$ molecules cm^{-2}). Even at peak sensitivity, the instrument has an error of 30% per retrieval. This error compounds to more than 100% over areas with lower signals. The anticipated changes in HCHO due to oil palm expansion are therefore near the detection limits of the OMI instrument. Furthermore, the OMI sensor has been slowly degrading with time, causing a significant drop in data density since mid 2007 (Gonzalez Abad et al., 2015) due to an issue known as the "row anomaly".
15 Instrument degradation is apparent in plots of annual average OMI HCHO, shown in Figure 14. Figure 14 suggests that HCHO concentrations have increased over SEA from 2005 through 2014, but that this is consistent with an overall increase in background HCHO that is not limited to SEA. This issue with instrument sensitivity, combined with a large decrease in the number of available observations makes it difficult to identify a significant trend in the HCHO satellite record. Figure 15 shows the monthly mean HCHO columns from OMI across all three selected land regions, as well as a LOWESS fit of the
20 data with the shaded regions representing the 95% confidence interval obtained through a LOWESS block bootstrapping scheme (Cleveland, 1979). The measured HCHO over the forest and palm regions are both generally higher than over the ocean. The LOWESS analysis shows that HCHO concentrations are highest over the palm region, with a mean difference of ~0.6 x 10^{15} molecules cm^{-2}, slightly lower than but of similar magnitude to the difference expected from our model simulations. This supports the results of our simulations, but also demonstrates how challenging it is to identify this signal
25 from satellite observations. While the LOWESS analysis also suggests that the OMI HCHO column concentrations across the region increased over this time period, much of this may be driven by the row anomaly and we do not see evidence for significant palm plantation growth within our limited palm region selected in Figure 13.

There is large uncertainty with regard to the distribution and application of fertilizer on oil palm plantations (Mohd et al.
30 2015, Fowler et al. 2011) and industrial emissions of NO$_x$ associated with palm processing facilities (Hewitt et al., 2009). OMI NO$_2$ tropospheric retrievals are shown in Figure 16. Similar to the HCHO retrievals, both monthly mean columns and the LOWESS fit with 95% confidence intervals are shown. The NO$_2$ columns above the palm region are generally higher relative to the forest region, but again there is no increasing difference over time. This is consistent with a lack of significant growth in fertilizer application or industrial emissions over the oil palm region selected in Figure 13. The constant palm-

forest difference of 10^{14} molecules cm^{-2} (~25%) agrees with our modeled analysis, which shows surface concentrations that differ by ~29% in this region, related to elevated anthropogenic NO$_x$ emissions. This suggests that we are not missing major palm-related sources of NO$_x$ emissions (fertilizer or industrial processing) in our simulation. The constant increase in retrieved NO$_2$ concentrations over all three regions is consistent with Geddes et al. (2015b), who show a broad increasing trend in NO$_2$ across all of northern Borneo, possibly due to warmer surface temperatures, and transport from urban regions.

The satellite-derived signal in tropospheric ozone from oil palm development near Kuala Lumpur is not apparent against the background of urban development. Even though there are significant changes in the local ozone concentrations, too many confounding sources exist to identify the oil palm signal. Fires in SEA dominate the measured AOD, with an additional contribution from urban sources (Cohen and Lecoeur, 2015). Since the AOD measurement is a net observation of extinction from all aerosols at all altitudes, detecting changes in surface-level SOA is not straightforward. It is therefore challenging to identify the impact of oil palm expansion on air quality in SEA with the current constellation of polar-orbiting satellites.

In light of this result, it is important to consider the monitoring capabilities of future observing systems, such as the North American geostationary mission TEMPO (Chance et al. 2013). Geostationary observations offer more frequent sampling of the diurnal cycle, which may enable a separation of source signatures (e.g. urban, fire, biogenic, etc.) and a better identification of perturbations associated with land use change. In terms of HCHO measurements, TEMPO has a similar precision to that of the OMI sensor (10^{16} molecules cm^{-2}). However, TEMPO will have much smaller spatial footprint (8x4.5 km) as compared to OMI (14x24 km), and will sample HCHO three times daily, as opposed to the once daily measurements from OMI. The combination of these factors will likely make changes in the emissions of HCHO and its precursors more detectable, if they occur within the geostationary viewing field. Our results indicate that the instrument precision and footprint size are the most important limiting factor in detection of the perturbation associated with oil palm plantations with the current suite of satellite observations.

5. Conclusions

In this study, we simulate the impact of recent and near-term projected oil palm expansion across SEA on air quality. We go beyond previous work by consistently treating the impact of land use change on a suite of land-atmosphere exchange processes relevant to atmospheric chemistry. Our simulations suggest that oil palm plantation expansion in the region has had a significant impact on air quality. As oil palm expansion continues, the potential impact on surface O$_3$ concentrations is significant. The predicted ozone changes are largely due to increasing isoprene emissions. Locally however, increases in depositional velocities counteract these elevated emissions. If the oil palm crop expansion continues unabated, near-term future ozone concentrations in urban regions could be up to 30% higher (compared to the no palm scenario) due to the plantations alone. Exposure to ozone is a significant cause of premature mortality, responsible for more than 200,000 deaths

globally in 2013 (Forouzanfar et al., 2015). The increase in ozone attributable to oil palm plantations has the potential to bring many regions in SEA (including the dense urban areas of Singapore and Kuala Lumpur) further above WHO recommended threshold concentrations. The increase in particulate matter due to biogenic secondary organic aerosol formation presents an additional health concern. Over Singapore, our results indicate that the addition of oil palm plantations

5 contributes 9% of the target WHO recommended ozone concentrations, and 4% of the recommended 24 hour particulate matter concentrations. This is on the same order as the seasonal average predicted contribution of fires to the same particulate matter air quality targets (~8%) (Marlier et al., 2015a). This work illustrates that in trying to reach local air quality objectives, it is important to consider the impacts of local land use change.

10 In this study we do not include the potential air quality impacts associated with local oil palm processing plants and prescribed burning of the fields. These are likely to lead to additional impacts on regional air quality, some of which have been described by Austin et al. (2015), Marlier et al. (2015a), and Hewitt et al. (2009). We also have limited constraints on how depositional fluxes are altered by land use transitions, and the fertilization practices for oil palm. However our simulation of NO_x and ozone deposition in the region appears to be broadly consistent within the range measurements from

15 the OP3 campaign.

Though the rapid oil palm expansion in SEA has led to substantial changes in the concentration of many atmospheric species, including HCHO, O_3, and aerosols, many of these changes occur in areas with high fire and urban activity. Because of this, the signal of oil palm impacts on air quality is difficult to disentangle from the satellite record. This issue of strong

20 confounding sources is compounded with issues of instrument sensitivity and degradation over time. This study suggests that future observing systems will require better sensitivities and stability to capture the impacts of land use change on air quality.

This work is an example of the impact of significant land use conversion on the regional scale. The growing pressures on the global food supply are likely to lead to further land conversions to support agricultural activity in the coming decades. Future

25 atmospheric composition will respond to these changes, with implications for air quality and climate, and will remain important to monitor and understand.

Acknowledgements

This work was supported by NSF (AGS-1238109).

References

Ashworth, K., G. Folberth, C. N. Hewitt, and O. Wild. "Impacts of near-Future Cultivation of Biofuel Feedstocks on Atmospheric Composition and Local Air Quality." Atmos. Chem. Phys. 12, no. 2 (January 19, 2012): 919–39. doi:10.5194/acp-12-919-2012.

Austin, Kemen G., Prasad S. Kasibhatla, Dean L. Urban, Fred Stolle, and Jeffrey Vincent. "Reconciling Oil Palm Expansion and Climate Change Mitigation in Kalimantan, Indonesia." PLoS ONE 10, no. 5 (May 26, 2015): e0127963. doi:10.1371/journal.pone.0127963.

Bey, Isabelle, Daniel J. Jacob, Robert M. Yantosca, Jennifer A. Logan, Brendan D. Field, Arlene M. Fiore, Qinbin Li, Honguy Y. Liu, Loretta J. Mickley, and Martin G. Schultz. "Global Modeling of Tropospheric Chemistry with Assimilated Meteorology: Model Description and Evaluation." Journal of Geophysical Research: Atmospheres 106, no. D19 (October 16, 2001): 23073–95. doi:10.1029/2001JD000807.

Bak, J., X. Liu, et al. "Validation of OMI Total Ozone Retrievals from the SAO Ozone Profile Algorithm and Three Operational Algorithms with Brewer Measurements." Atmos. Chem. Phys. 15, no. 2 (January 19, 2015): 667–83. doi:10.5194/acp-15-667-2015.

Boersma, K. F., et al. "An Improved Tropospheric NO2 Column Retrieval Algorithm for the Ozone Monitoring Instrument." Atmos. Meas. Tech. 4, no. 9 (September 16, 2011): 1905–28. doi:10.5194/amt-4-1905-2011.

Carlson, Kimberly M., Lisa M. Curran, Gregory P. Asner, Alice McDonald Pittman, Simon N. Trigg, and J. Marion Adeney. "Carbon Emissions from Forest Conversion by Kalimantan Oil Palm Plantations." Nature Climate Change 3, no. 3 (March 2013): 283–87. doi:10.1038/nclimate1702.

Chance, Kelly, Xiong Liu, Raid M. Suleiman, David E. Flittner, Jassim Al-Saadi, Scott J. Janz, "Tropospheric emissions: Monitoring of pollution (TEMPO)," Proceedings of SPIE, Vol. 8866, 'Earth Observing Systems XVIII, 88660D (September 23, 2013),' San Diego, CA, USA, Aug. 25, 2013, URL:https://www.cfa.harvard.edu/atmosphere/publications/TEMPO-SPIE-2013-24aug2013.pdf

Cleveland, William S. "Robust Locally Weighted Regression and Smoothing Scatterplots." Journal of the American Statistical Association 74, no. 368 (1979): 829–36.

Cohen, J. B., and E. Lecoeur. "Decadal-Scale Relationship between Measurements of Aerosols, Land-Use Change, and Fire over Southeast Asia." Atmos. Chem. Phys. Discuss. 15, no. 19 (October 6, 2015): 26895–957. doi:10.5194/acpd-15-26895-2015.

5   Fan, Y., O. Roupsard, M. Bernoux, G. Le Maire, O. Panferov, M. M. Kotowska, and A. Knohl. "A Sub-Canopy Structure for Simulating Oil Palm in the Community Land Model (CLM-Palm): Phenology, Allocation and Yield." Geosci. Model Dev. 8, no. 11 (November 26, 2015): 3785–3800. doi:10.5194/gmd-8-3785-2015.

Fitzherbert, Emily B., Matthew J. Struebig, Alexandra Morel, Finn Danielsen, Carsten A. Brühl, Paul F. Donald, and Ben
10 Phalan. "How Will Oil Palm Expansion Affect Biodiversity?" Trends in Ecology & Evolution 23, no. 10 (October 2008): 538–45. doi:10.1016/j.tree.2008.06.012.

Forouzanfar, Mohammad H, Lily Alexander, H Ross Anderson, Victoria F Bachman, Stan Biryukov, Michael Brauer, Richard Burnett, et al. "Global, Regional, and National Comparative Risk Assessment of 79 Behavioural, Environmental and
15 Occupational, and Metabolic Risks or Clusters of Risks in 188 Countries, 1990–2013: A Systematic Analysis for the Global Burden of Disease Study 2013." The Lancet. Accessed September 14, 2015. doi:10.1016/S0140-6736(15)00128-2.

Fowler, D., E. Nemitz, P. Misztal, C. Di Marco, U. Skiba, J. Ryder, C. Helfter, et al. "Effects of Land Use on Surface-Atmosphere Exchanges of Trace Gases and Energy in Borneo: Comparing Fluxes over Oil Palm Plantations and a
20 Rainforest." Philosophical Transactions of the Royal Society B: Biological Sciences 366, no. 1582 (November 27, 2011): 3196–3209. doi:10.1098/rstb.2011.0055.

Fu, Tzung-May, Daniel J. Jacob, Paul I. Palmer, Kelly Chance, Yuxuan X. Wang, Barbara Barletta, Donald R. Blake, Jenny C. Stanton, and Michael J. Pilling. "Space-Based Formaldehyde Measurements as Constraints on Volatile Organic
25 Compound Emissions in East and South Asia and Implications for Ozone." Journal of Geophysical Research: Atmospheres 112, no. D6 (March 27, 2007): D06312. doi:10.1029/2006JD007853.

Fuller, Douglas O. "MODIS Data Used to Study 2002 Fires in Kalimantan, Indonesia." Eos, Transactions American Geophysical Union 84, no. 20 (May 20, 2003): 189–92. doi:10.1029/2003EO200001.
30
Geddes, J. A., Heald, C. L., Silva, S. J., and Martin, R. V. (2015a): Land cover change impacts on atmospheric chemistry: simulating projected large-scale tree mortality in the United States, Atmos. Chem. Phys. Discuss., 15, 29303-29345, doi:10.5194/acpd-15-29303-2015a

Geddes J.A., Martin RV, Boys BL, and van Donkelaar A (2015b), Long term trends worldwide in ambient NO_2 concentrations inferred from satellite observations. Environmental Health Perspectives. DOI:10.1289/ehp.1409567

5   González Abad, G., X. Liu, K. Chance, H. Wang, T. P. Kurosu, and R. Suleiman. "Updated Smithsonian Astrophysical Observatory Ozone Monitoring Instrument (SAO OMI) Formaldehyde Retrieval." Atmos. Meas. Tech. 8, no. 1 (January 5, 2015): 19–32. doi:10.5194/amt-8-19-2015.

Guenther, A., T. Karl, P. Harley, C. Wiedinmyer, P. I. Palmer, and C. Geron. "Estimates of Global Terrestrial Isoprene Emissions Using MEGAN (Model of Emissions of Gases and Aerosols from Nature)." Atmos. Chem. Phys. 6, no. 11
10   (August 2, 2006): 3181–3210. doi:10.5194/acp-6-3181-2006.

Guenther, A. B., X. Jiang, C. L. Heald, T. Sakulyanontvittaya, T. Duhl, L. K. Emmons, and X. Wang. "The Model of Emissions of Gases and Aerosols from Nature Version 2.1 (MEGAN2.1): An Extended and Updated Framework for Modeling Biogenic Emissions." Geosci. Model Dev. 5, no. 6 (November 26, 2012): 1471–92. doi:10.5194/gmd-5-1471-
15   2012.

Heald, Colette L., and Dominick V. Spracklen. "Land Use Change Impacts on Air Quality and Climate." Chemical Reviews 115, no. 10 (May 27, 2015): 4476–96. doi:10.1021/cr500446g.

20   Hewitt, C. N., A. R. MacKenzie, P. Di Carlo, C. F. Di Marco, J. R. Dorsey, M. Evans, D. Fowler, et al. "Nitrogen Management Is Essential to Prevent Tropical Oil Palm Plantations from Causing Ground-Level Ozone Pollution." Proceedings of the National Academy of Sciences 106, no. 44 (2009): 18447–51.

Hewitt, C. N., J. D. Lee, A. R. MacKenzie, M. P. Barkley, N. Carslaw, G. D. Carver, N. A. Chappell, et al. "Overview:
25   Oxidant and Particle Photochemical Processes above a South-East Asian Tropical Rainforest (the OP3 Project): Introduction, Rationale, Location Characteristics and Tools." Atmos. Chem. Phys. 10, no. 1 (January 12, 2010): 169–99. doi:10.5194/acp-10-169-2010.

Hudman, R. C., Moore, N. E., Mebust, A. K., Martin, R. V, Russell, A. R., Valin, L. C. and Cohen, R. C.: Steps towards a
30   mechanistic model of global soil nitric oxide emissions: implementation and space based-constraints, Atmos. Chem. Phys., 12(16), 7779–7795, doi:10.5194/acp-12-7779-2012, 2012.

Jiang, Z., J. R. Worden, D. B. A. Jones, J.-T. Lin, W. W. Verstraeten, and D. K. Henze. "Constraints on Asian Ozone Using Aura TES, OMI and Terra MOPITT." Atmos. Chem. Phys. 15, no. 1 (January 8, 2015): 99–112. doi:10.5194/acp-15-99-2015.

5   Kim, P. S., et al. "Global ozone–CO Correlations from OMI and AIRS: Constraints on Tropospheric Ozone Sources." Atmos. Chem. Phys. 13, no. 18 (September 17, 2013): 9321–35. doi:10.5194/acp-13-9321-2013.

Langford, B., P. K. Misztal, E. Nemitz, B. Davison, C. Helfter, T. A. M. Pugh, A. R. MacKenzie, S. F. Lim, and C. N. Hewitt. "Fluxes and Concentrations of Volatile Organic Compounds from a South-East Asian Tropical Rainforest."
10 Atmospheric Chemistry and Physics 10, no. 17 (September 7, 2010): 8391–8412. doi:10.5194/acp-10-8391-2010.

Lawrence, David M, Keith W Oleson, Mark G Flanner, Peter E Thornton, Sean C Swenson, Peter J Lawrence, Xubin Zeng, et al. "Parameterization Improvements and Functional and Structural Advances in Version 4 of the Community Land Model." Journal of Advances in Modeling Earth Systems 3, no. 3 (March 19, 2011). doi:10.1029/2011MS000045.

Mao, Jingqiu, Fabien Paulot, Daniel J. Jacob, Ronald C. Cohen, John D. Crounse, Paul O. Wennberg, Christoph A. Keller, Rynda C. Hudman, Michael P. Barkley, and Larry W. Horowitz. "Ozone and Organic Nitrates over the Eastern United States: Sensitivity to Isoprene Chemistry." Journal of Geophysical Research: Atmospheres 118, no. 19 (October 16, 2013): 2013JD020231. doi:10.1002/jgrd.50817.

Marlier, Miriam E., Ruth S. DeFries, Apostolos Voulgarakis, Patrick L. Kinney, James T. Randerson, Drew T. Shindell, Yang Chen, and Greg Faluvegi. "El Nino and Health Risks from Landscape Fire Emissions in Southeast Asia." Nature Climate Change 3, no. 2 (February 2013): 131–36. doi:10.1038/nclimate1658.

25 Marlier, Miriam E., Ruth S. DeFries, Patrick S. Kim, David L. A. Gaveau, Shannon N. Koplitz, Daniel J. Jacob, Loretta J. Mickley, Belinda A. Margono, and Samuel S. Myers. "Regional Air Quality Impacts of Future Fire Emissions in Sumatra and Kalimantan." Environmental Research Letters 10, no. 5 (2015a): 054010. doi:10.1088/1748-9326/10/5/054010.

Marlier, Miriam E., Ruth DeFries, Derric Pennington, Erik Nelson, Elsa M. Ordway, Jeremy Lewis, Shannon N. Koplitz,
30 and Loretta J. Mickley. "Future Fire Emissions Associated with Projected Land Use Change in Sumatra." Global Change Biology 21, no. 1 (January 1, 2015b): 345–62. doi:10.1111/gcb.12691.

Miettinen, Jukka, Chenghua Shi, Wee Juan Tan, and Soo Chin Liew. "2010 Land Cover Map of Insular Southeast Asia in 250-M Spatial Resolution." Remote Sensing Letters 3, no. 1 (2012): 11–20. doi:10.1080/01431161.2010.526971.

Misztal, P. K., E. Nemitz, B. Langford, C. F. Di Marco, G. J. Phillips, C. N. Hewitt, A. R. MacKenzie, et al. "Direct Ecosystem Fluxes of Volatile Organic Compounds from Oil Palms in South-East Asia." Atmos. Chem. Phys. 11, no. 17 (September 2, 2011): 8995–9017. doi:10.5194/acp-11-8995-2011.

Mohd Kusin, Faradiella, Nurul Izzati Mat Akhir, Ferdaus Mohamat-Yusuff, and Muhamad Awang. "The Impact of Nitrogen Fertilizer Use on Greenhouse Gas Emissions in an Oil Palm Plantation Associated with Land Use Change." Atmósfera 28, no. 4. (2015)

10   Olivier, J.G.J. and J.J.M. Berdowski, Global emissions sources and sinks. In: Berdowski, J., Guicherit, R. and B.J. Heij (eds.) The Climate System, pp. 33-78. A. A. Balkema Publishers/Swets & Zeitlinger Publishers, Lisse, The Netherlands., 2001

Park, Rokjin J., Daniel J. Jacob, Naresh Kumar, and Robert M. Yantosca. "Regional Visibility Statistics in the United States:
15   Natural and Transboundary Pollution Influences, and Implications for the Regional Haze Rule." Atmospheric Environment 40, no. 28 (September 2006): 5405–23. doi:10.1016/j.atmosenv.2006.04.059.

Pike, R. C., J. D. Lee, P. J. Young, G. D. Carver, X. Yang, N. Warwick, S. Moller, et al. "NOx and O3 above a Tropical Rainforest: An Analysis with a Global and Box Model." Atmos. Chem. Phys. 10, no. 21 (November 11, 2010): 10607–20.
20   doi:10.5194/acp-10-10607-2010.

Pye, H. O. T., H. Liao, S. Wu, L. J. Mickley, D. J. Jacob, D. K. Henze, and J. H. Seinfeld, Effect of changes in climate and emissions on future sulfate-nitrate-ammonium aerosol levels in the United States, *J. Geophys. Res.*, 2009.

25   Pye, H. O. T., A. W. H. Chan, M. P. Barkley, and J. H. Seinfeld. "Global Modeling of Organic Aerosol: The Importance of Reactive Nitrogen (NOx and NO3)." Atmos. Chem. Phys. 10, no. 22 (November 30, 2010): 11261–76. doi:10.5194/acp-10-11261-2010.

Pye, H. O. T., and J. H. Seinfeld. "A Global Perspective on Aerosol from Low-Volatility Organic Compounds." Atmos.
30   Chem. Phys. 10, no. 9 (May 12, 2010): 4377–4401. doi:10.5194/acp-10-4377-2010.

Sayer, A. M., et al. "MODIS Collection 6 Aerosol Products: Comparison between Aqua's E-Deep Blue, Dark Target, and 'merged' Data Sets, and Usage Recommendations." Journal of Geophysical Research: Atmospheres, 2014, 2014JD022453. doi:10.1002/2014JD022453

Steinkamp, J. and Lawrence, M. G.: Improvement and evaluation of simulated global biogenic soil NO emissions in an AC-GCM, Atmos. Chem. Phys., 11(12), 6063–6082, doi:10.5194/acp-11-6063-2011, 2011.

5   Simone, N.W., M.E.J. Stettler, S.R.H. Barrett, Rapid estimation of global civil aviation emissions with uncertainty quantification, Transportation Research Part D: Transport and Environment, 25, 33-41, 2012.

Stettler, M.E.J., S. Eastham, S.R.H. Barrett, Air quality and public health impacts of UK airports. Part I: Emissions, Atmo. Environ., 45, 5415-5424, 2011.

Streets, D.G., T.C. Bond, G.R. Carmichael, S.D. Fernandes, Q. Fu, Z. Klimont, S.M. Nelson, N.Y. Tsai, M.Q. Wang, J-H. Woo, and K.F. Yarber, An inventory of gaseous and primary aerosol emissions in Asia in the year 2000, J. Geophys. Res, 108, D21, doi:10.1029/2002JD003093, 2003.

15   Streets, D.G, Q. Zhang, L. Wang, K. He, J. Hao, Y. Wu, Y. Tang, and G.C. Carmichael, Revisiting China's CO emissions after the Transport and Chemical Evolution over the Pacific (TRACE-P) mission: Synthesis of inventories, atmospheric modeling, and observations, J. Geophys. Res, 111, D14306, doi:10.1029/2006JD007118, 2006.

Trivitayanurak, W., P. I. Palmer, M. P. Barkley, N. H. Robinson, H. Coe, and D. E. Oram. "The Composition and Variability
20   of Atmospheric Aerosol over Southeast Asia during 2008." Atmos. Chem. Phys. 12, no. 2 (January 26, 2012): 1083–1100. doi:10.5194/acp-12-1083-2012.

United Nations, Department of Economic and Social Affairs, Population
Division (2011). World Population Prospects: The 2010 Revision, Volume I:
25   Comprehensive Tables. ST/ESA/SER.A/313.

van der Werf, G.R., J.T. Randerson, L. Giglio, G.J. Collatz,M. Mu, P.S. Kasibhatla, D.C. Morton, R.S. DeFries, Y. Jin, and T.T. van Leeuwen, Global fire emissions and the contribution of deforestation, savanna, forest, agricultural, and peat fires (1997–2009), Atm. Chem. Phys., Vol 10, 11707–11735, 2010.

Van Kraalingen, D. W. G, C. J Breure, and C. J. T Spitters. "Simulation of Oil Palm Growth and Yield." Agricultural and Forest Meteorology 46, no. 3 (May 1989): 227–44. doi:10.1016/0168-1923(89)90066-X.

Vinken, G. C. M., et al. "Worldwide Biogenic Soil NOx Emissions Inferred from OMI NO2 Observations." Atmos. Chem. Phys. 14, no. 18(September 30, 2014): 10363–81. doi:10.5194/acp-14 10363-2014.

Warwick, N. J., A. T. Archibald, K. Ashworth, J. Dorsey, P. M. Edwards, D. E. Heard, B. Langford, et al. "A Global Model Study of the Impact of Land-Use Change in Borneo on Atmospheric Composition." Atmospheric Chemistry and Physics 13, no. 18 (September 16, 2013): 9183–94. doi:10.5194/acp-13-9183-2013.

Wesely, M. L.: Parameterization of surface resistances to gaseous dry deposition in regional-scale numerical models, Atmos. Environ., 23(6), 1293–1304, doi:10.1016/0004-6981(89)90153-4, 1989.

Zhu, Lei, Daniel J. Jacob, Loretta J. Mickley, Eloïse A. Marais, Daniel S. Cohan, Yasuko Yoshida, Bryan N. Duncan, Gonzalo González Abad, and Kelly V. Chance. "Anthropogenic Emissions of Highly Reactive Volatile Organic Compounds in Eastern Texas Inferred from Oversampling of Satellite (OMI) Measurements of HCHO Columns." Environmental Research Letters 9, no. 11 (November 1, 2014): 114004. doi:10.1088/1748-9326/9/11/114004.

Figures
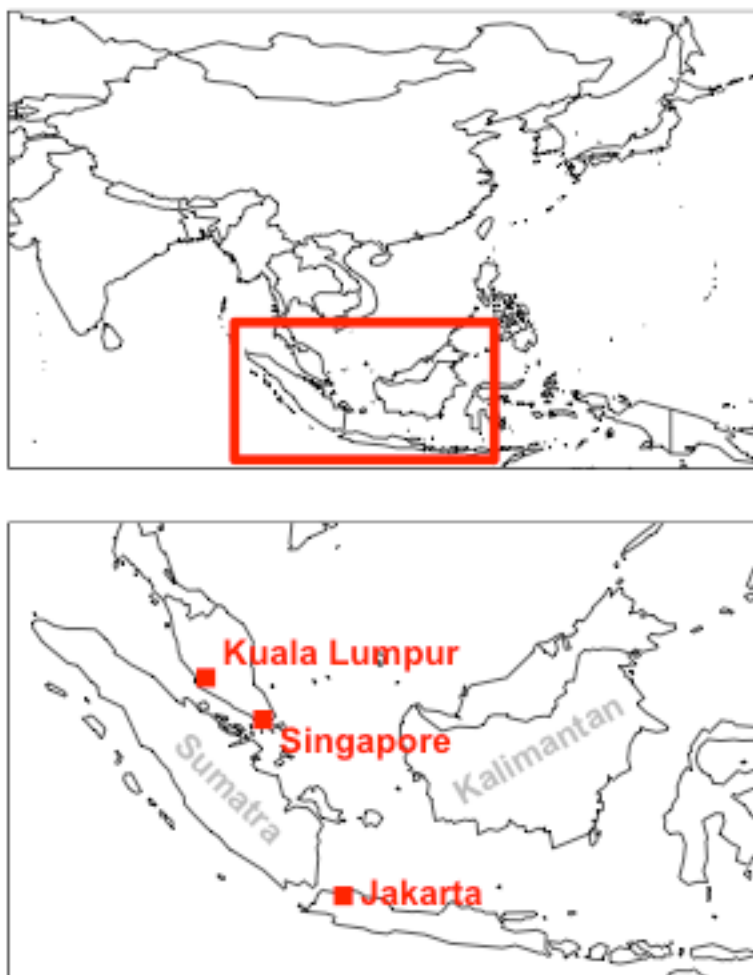
Figure 1: The nested GEOS-Chem Asian domain simulated at 0.5x 0.67 (top) and the particular region of interest explored in this work (bottom). The location of major regions discussed in the text are also shown.
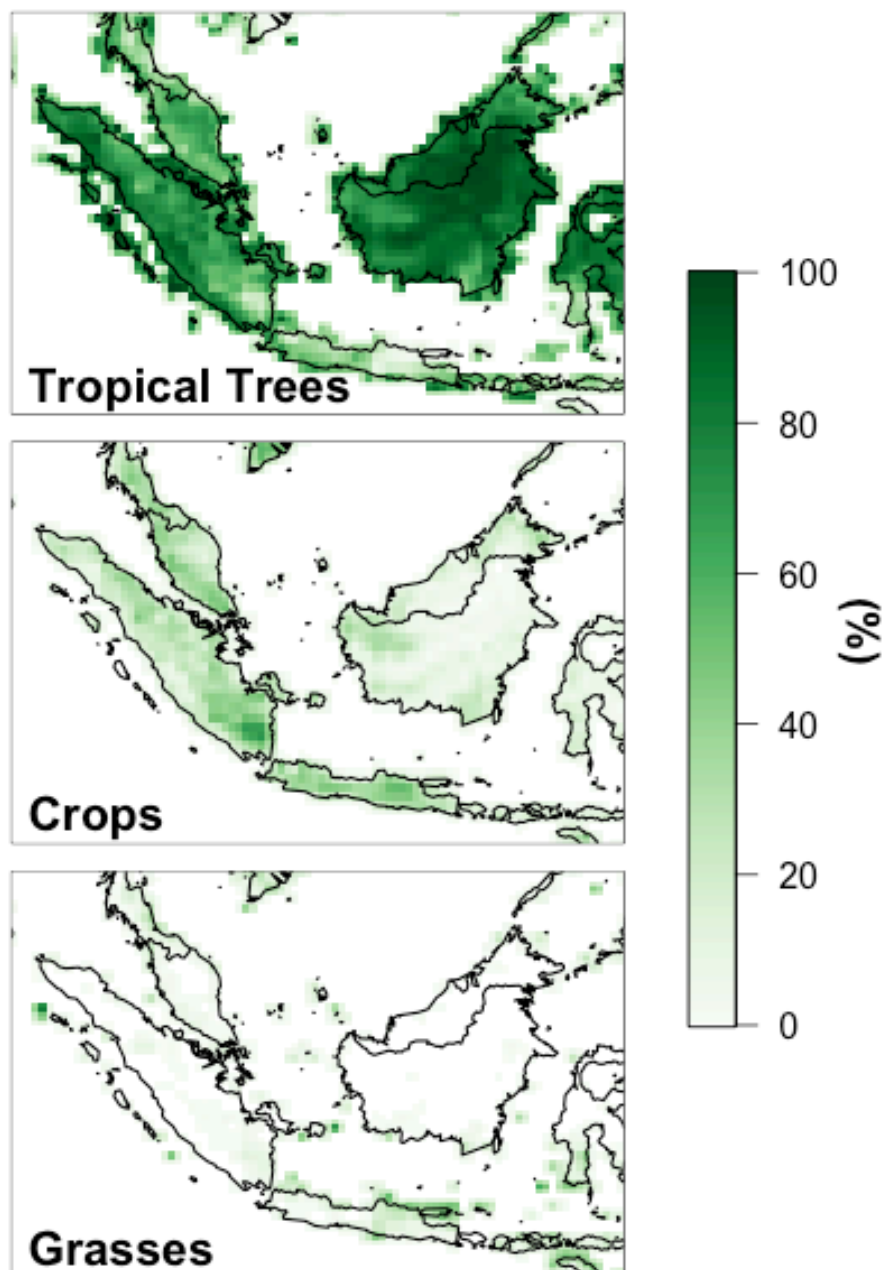
Figure 2: Percentage of vegetated area occupied by dominant vegetation classes in the No Palm scenario at the native 0.23˚x0.31˚ resolution.
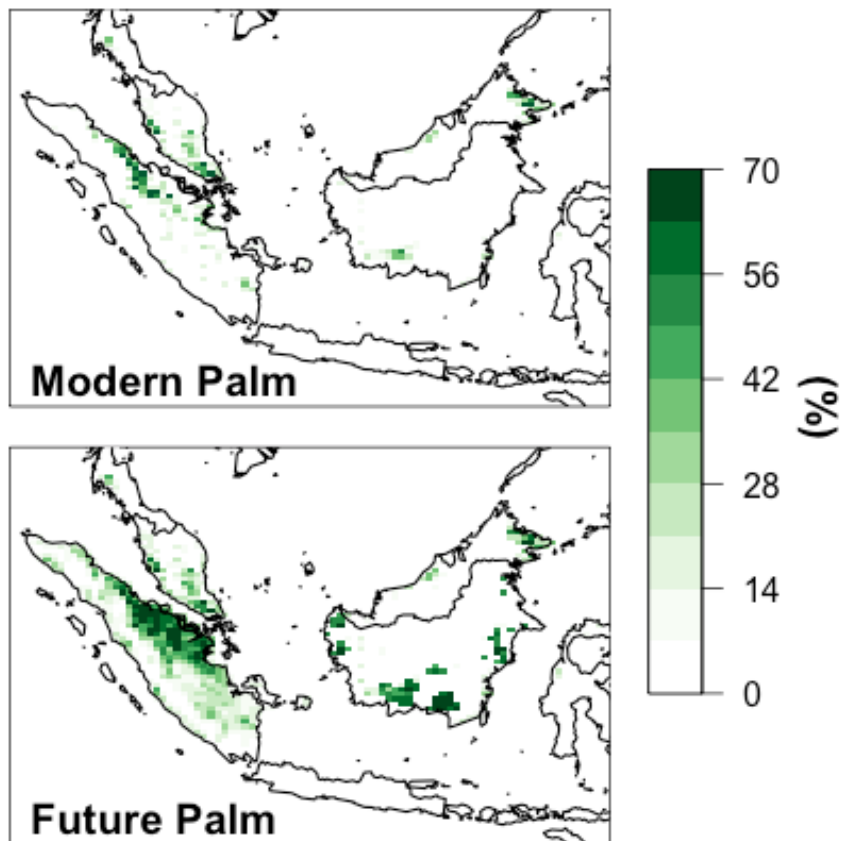
Figure 3: Percentage of vegetated area occupied by oil palm plantations for Modern (2010) and Future scenarios. Note that estimates for palm planatation increases from 2010 to the near-term future are only avaialble for Sumatra and Kalimantan; palm plantation coverage in other regions are assumed constant.
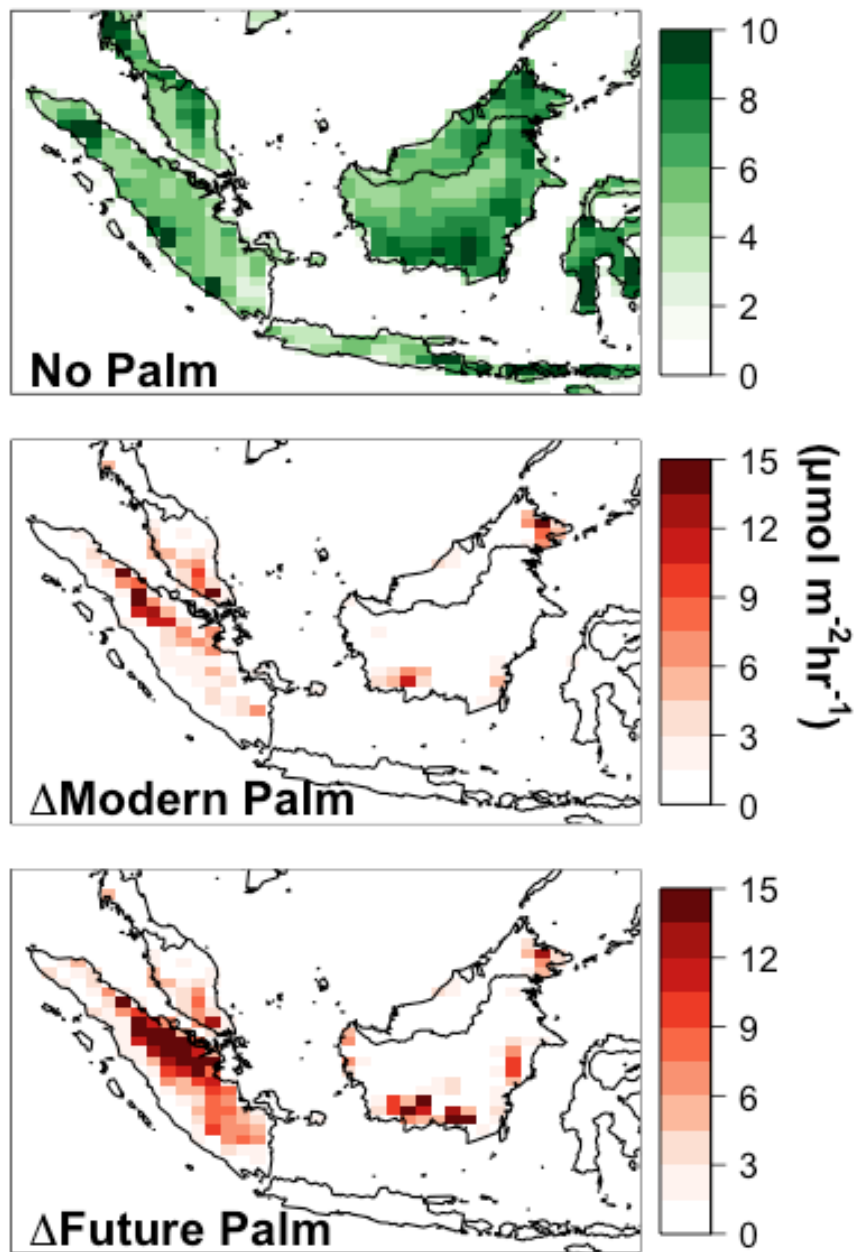
Figure 4: Annual mean simulated isoprene emissions over SEA (top) and the change due to Modern (middle) and Future (bottom) oil palm expansion.
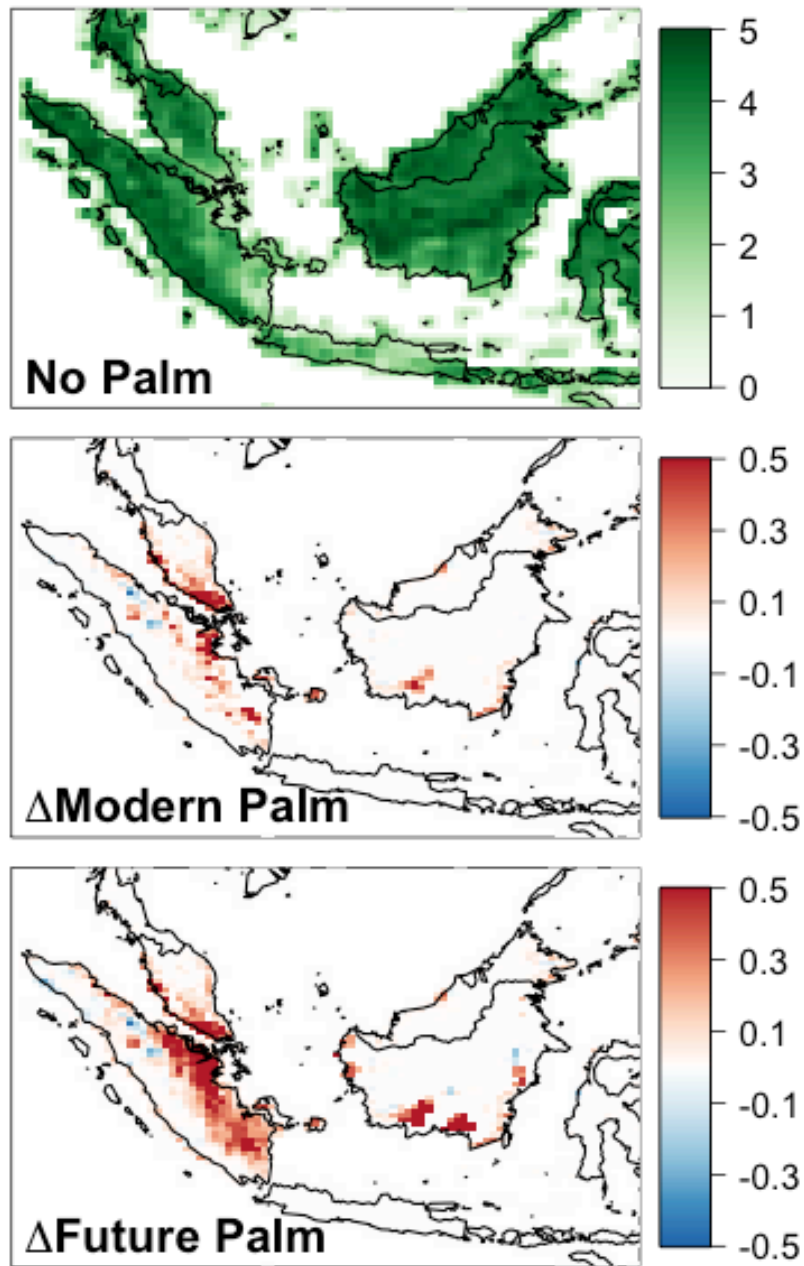
Figure 5: Annual average leaf area index (LAI) over SEA (top) and the change due to Modern (middle) and Future (bottom) palm expansion.
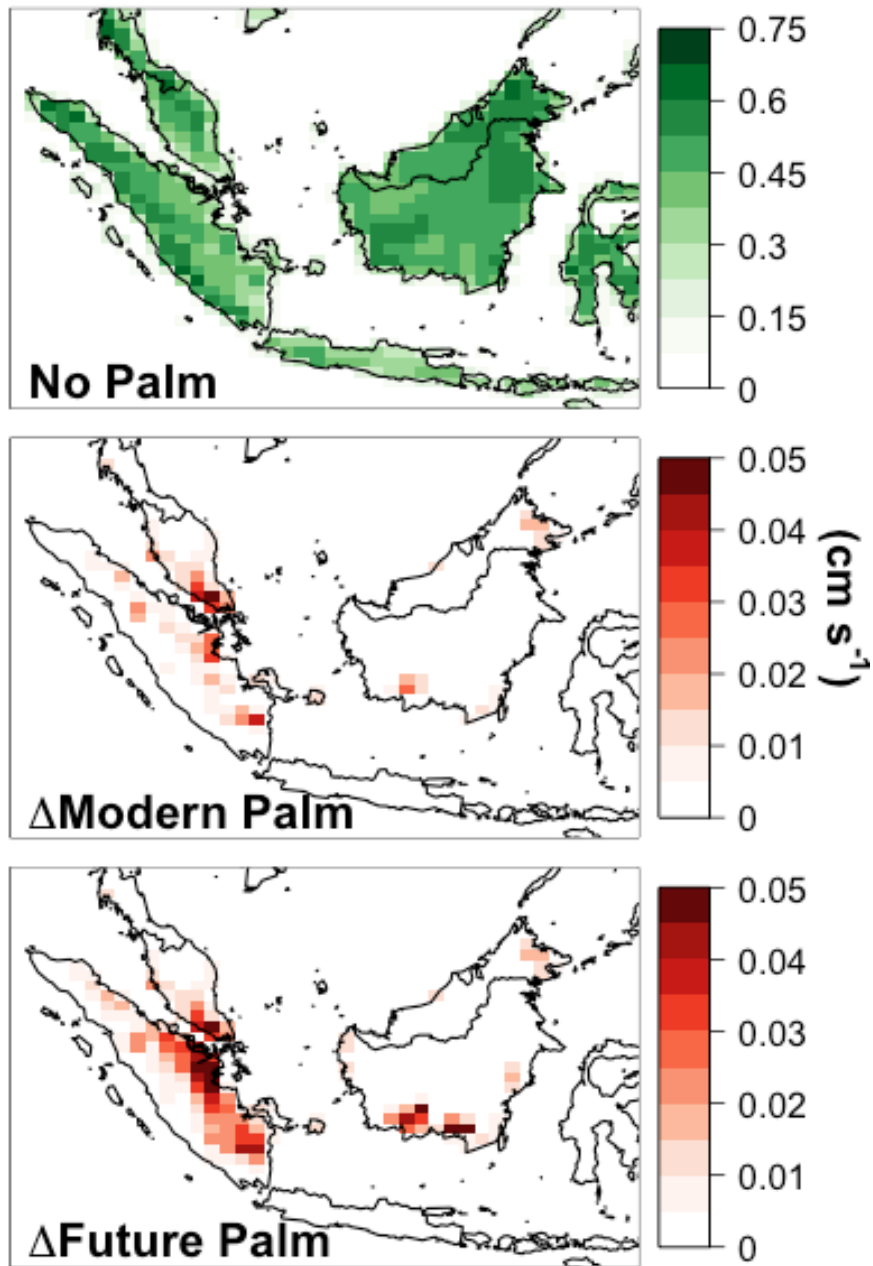
Figure 6: Annual average ozone dry deposition velocity over SEA (top) and the change due to Modern (middle) and Future (bottom) palm expansion.
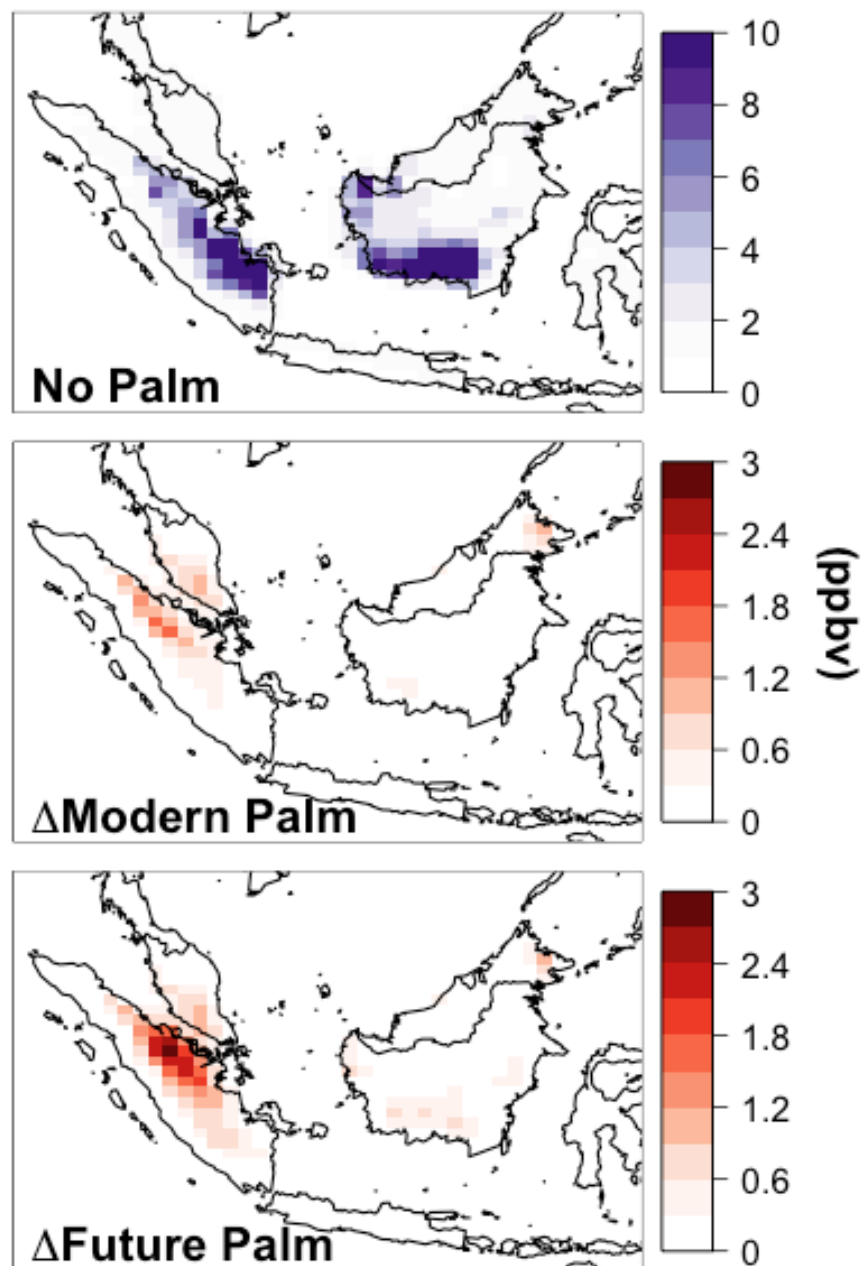
Figure 7: Annual average surface formaldehyde (HCHO) concentrations over SEA (top) and the change due to Modern (middle) and Future (bottom) palm expansion.
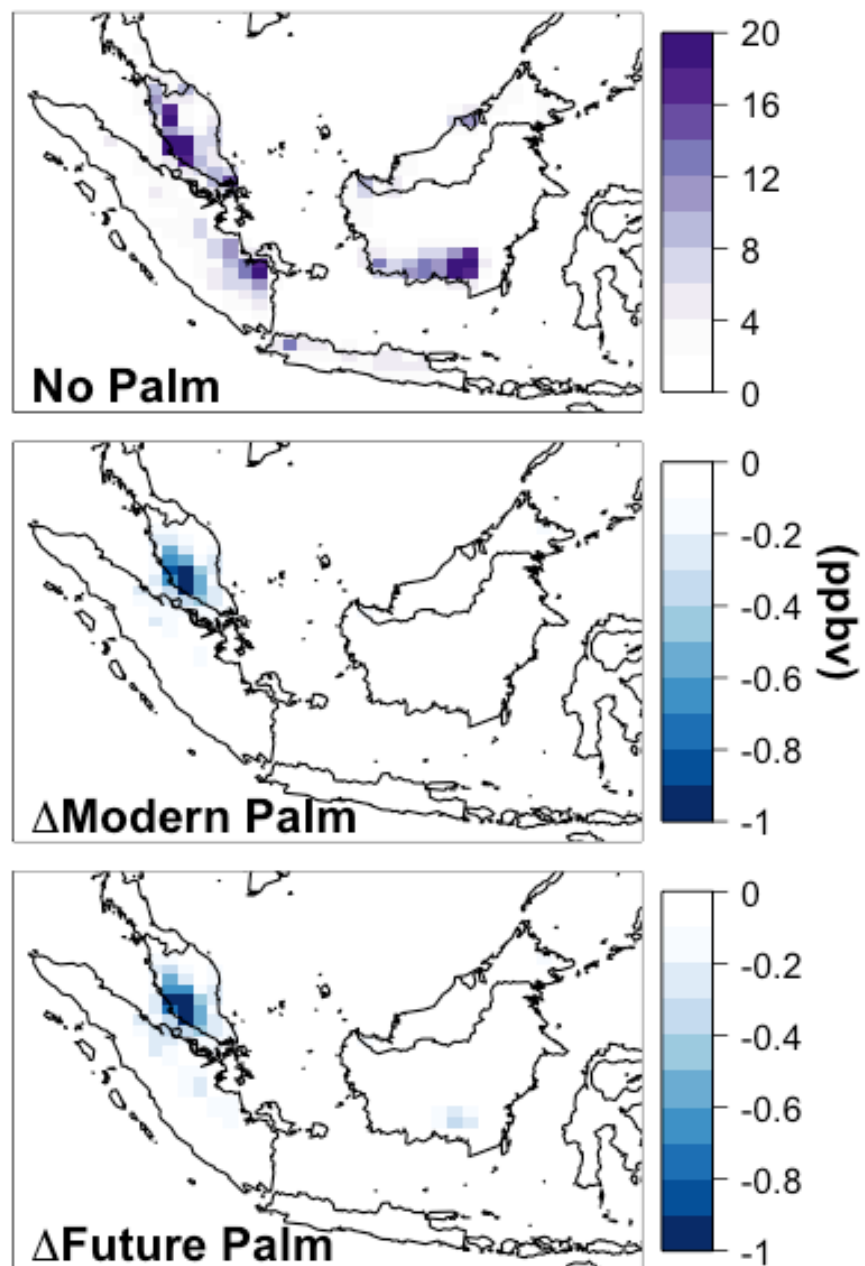
Figure 8: Annual average surface nitrogen oxides (NO$_x$) concentrations over SEA (top) and the change due to Modern (middle) and Future (bottom) palm expansion.
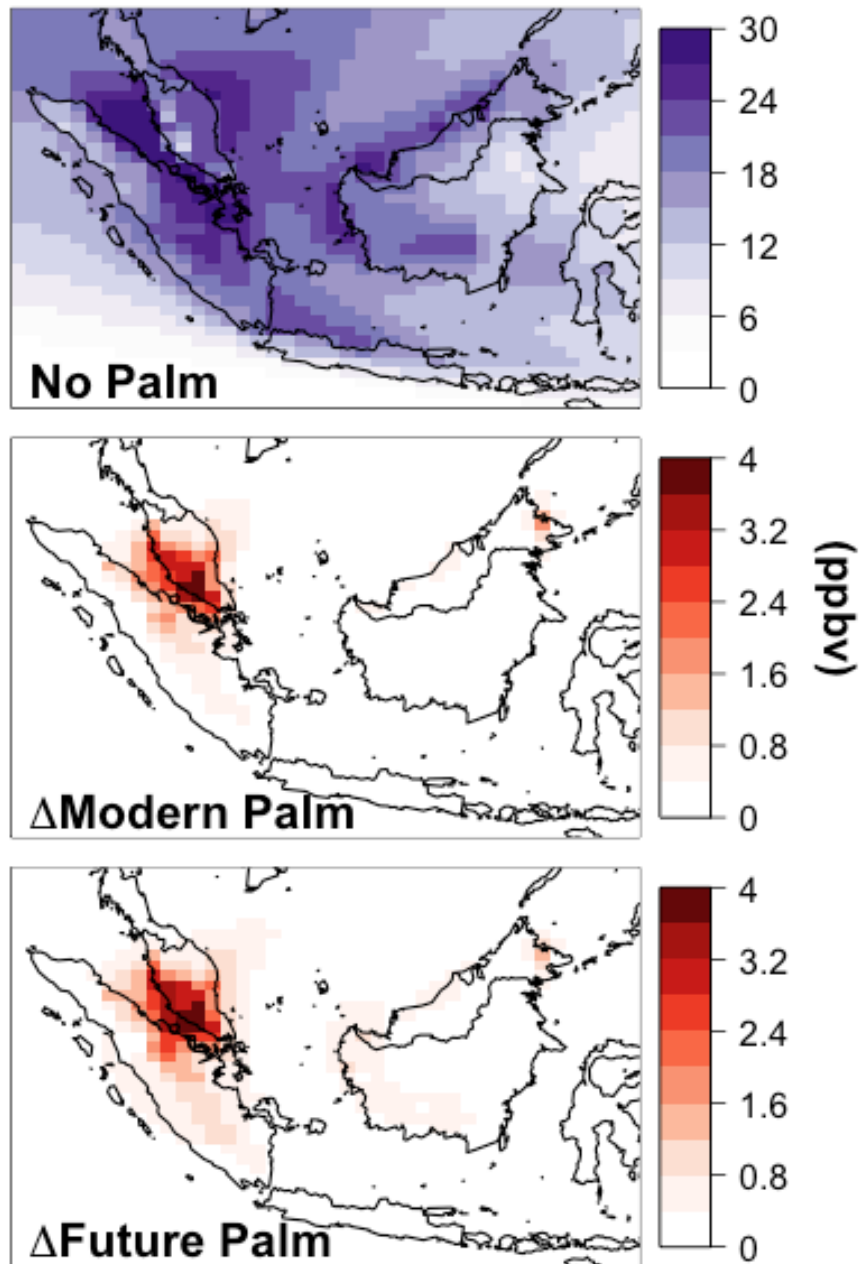
Figure 9: Annual average surface ozone concentrations over SEA (top) and the change due to Modern (middle) and Future (bottom) palm expansion.
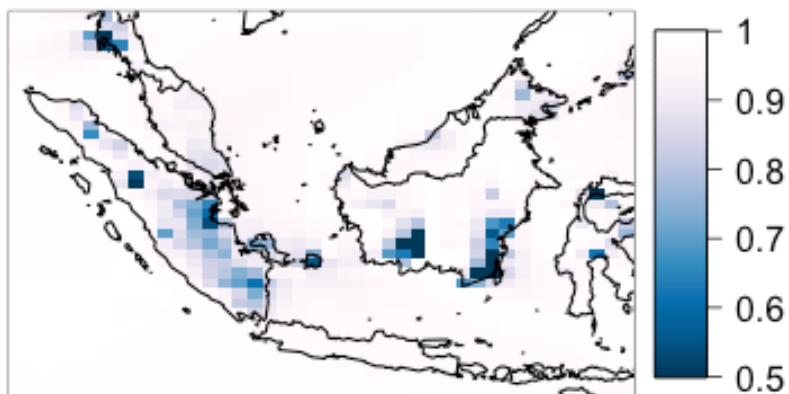
Figure 10: The ratio of the changes in ozone concentrations in the Modern Palm scenario compared to the changes in ozone in the BVOC-only simulation. Regions less than 1 show where increasing deposition velocities over palm plantations counteract some of the ozone increases driven by increasing isoprene emissions.
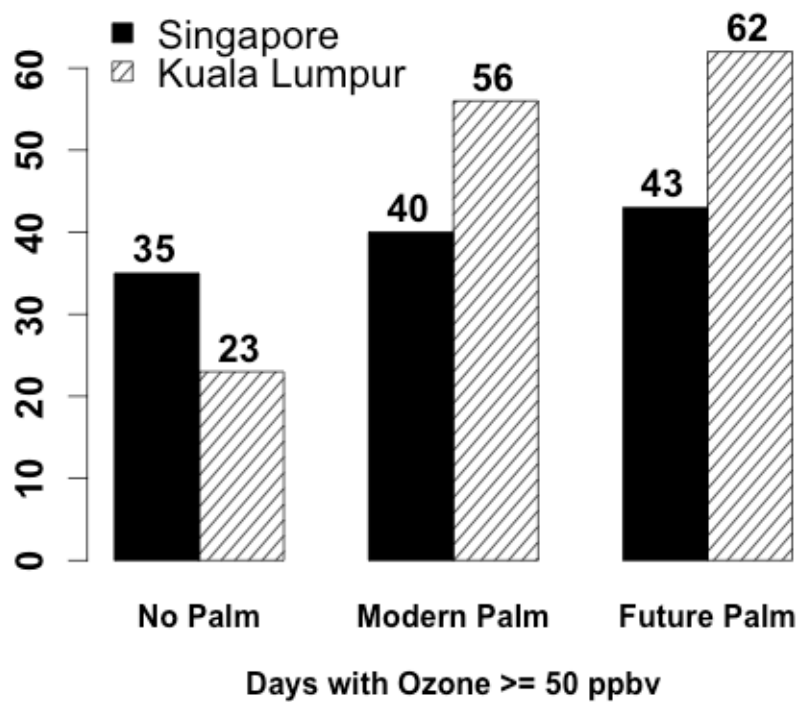
Figure 11: The number of days with simulated daily maximum 8-hour average surface ozone concentrations exceeding 50 ppbv over Singapore and Kuala Lumpur.
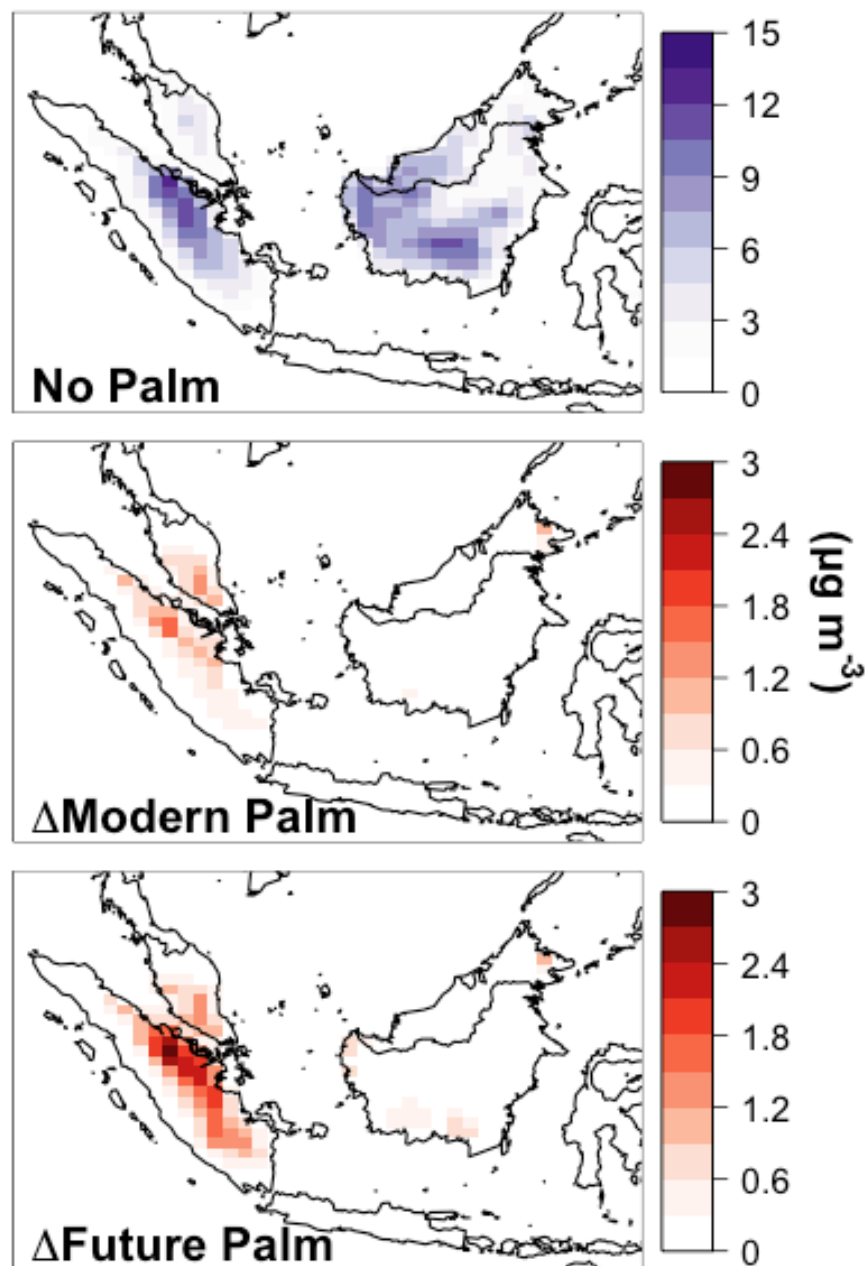
Figure 12: Annual average surface biogenic secondary organic aerosol (SOA) concentrations over SEA (top) and the change due to Modern (middle) and Future (bottom) palm expansion.
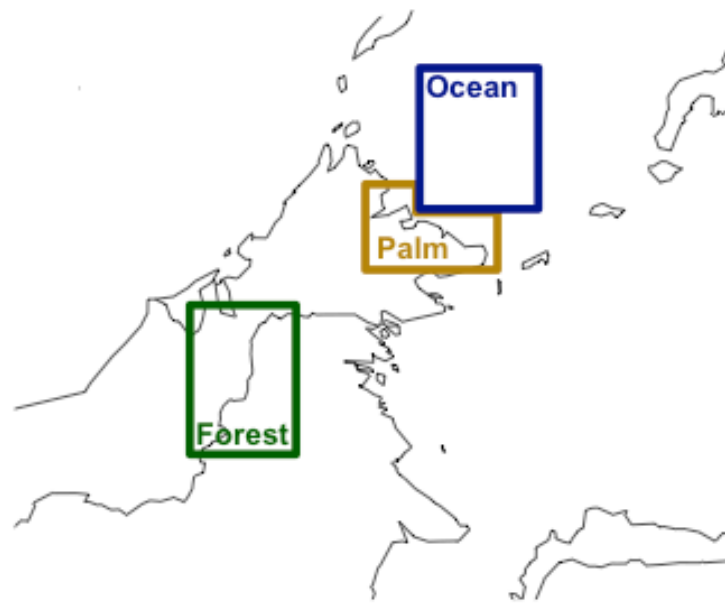
Figure 13: The three regions in northeastern Borneo used for the spatial filtering of the satellite data.
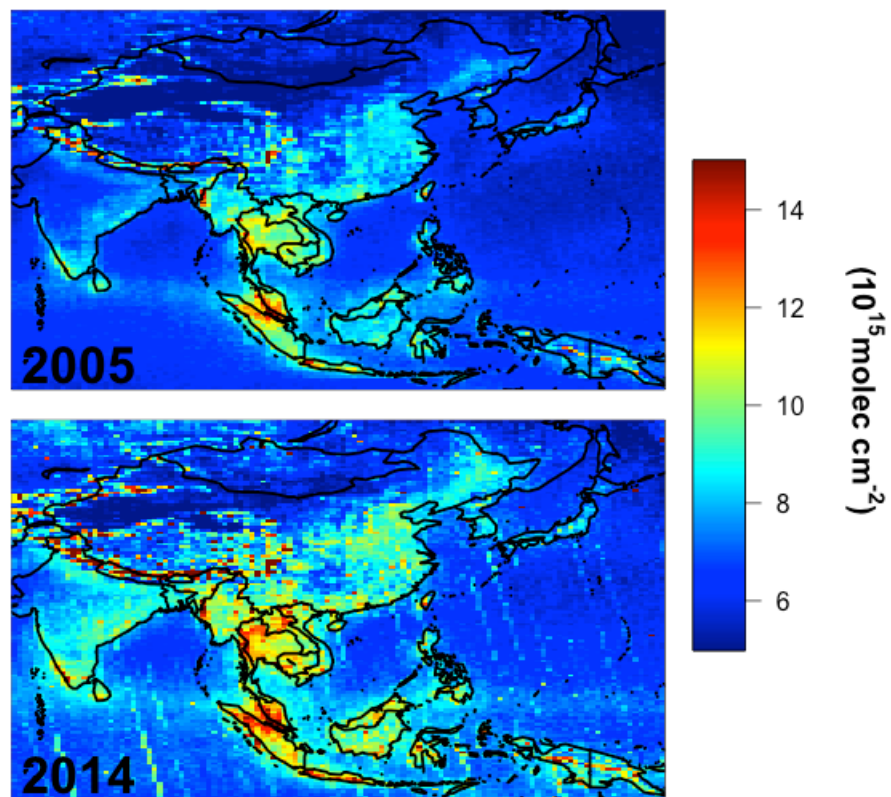
Figure 14: Annual average HCHO columns measured by the OMI instrument in 2005 and 2014.
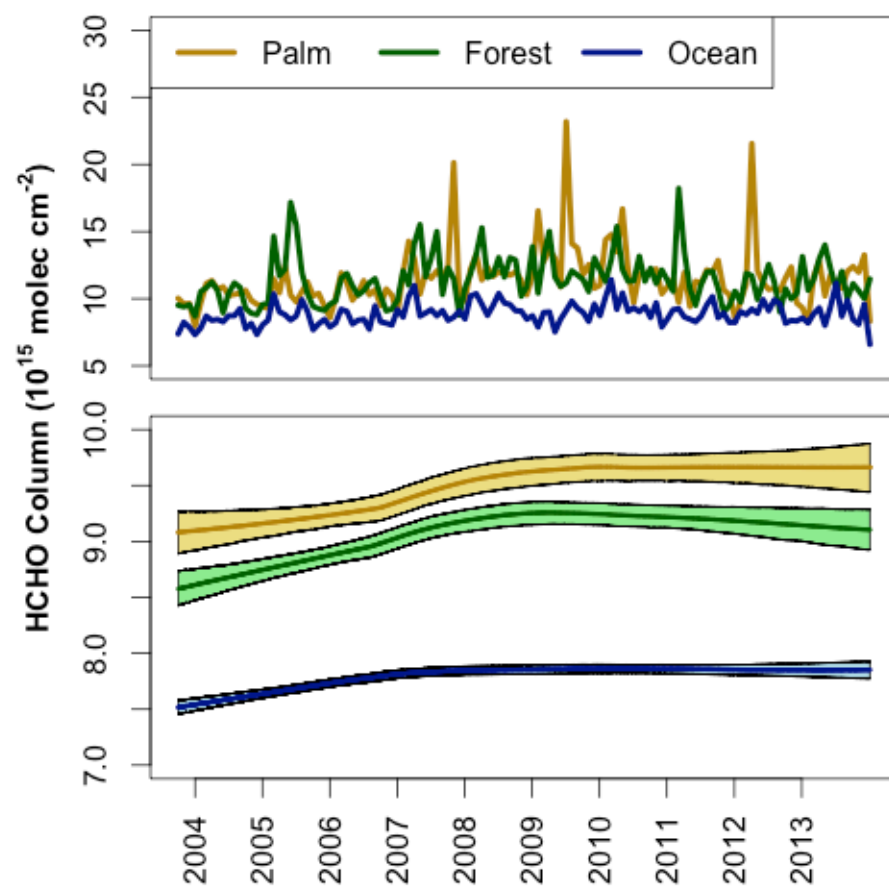
Figure 15: A monthly mean and LOWESS timeseries of HCHO from OMI in the three separate regions of northern Borneo (see Figure 13). The LOWESS shaded regions represent the 95% confidence interval.
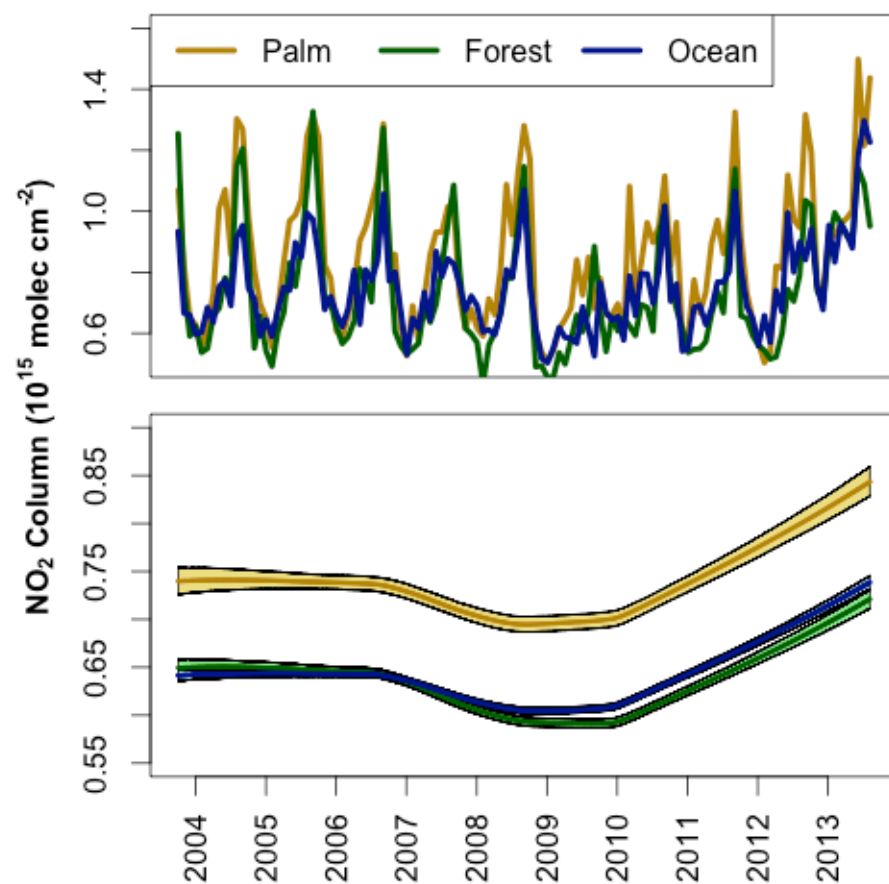
Figure 16: A monthly mean and LOWESS timeseries of NO₂ from OMI in the three separate regions of northern Borneo (see Figure 13). The LOWESS shaded regions represent the 95% confidence interval.